Industrial Chemistry Publication Series

Teknillisen kemian julkaisusarja

Espoo 2003 No. 16

KINETIC ANALYSIS OF TEMPERATURE-PROGRAMMED REACTIONS

Jaana Kanervo

Dissertation for the degree of Doctor of Science in Technology to be presented with due permission of the Department of Chemical Technology for public examination and debate in Auditorium Ke 2 (Komppa Auditorium) at Helsinki University of Technology (Espoo, Finland) on the 16th of October, 2003, at 12 o'clock noon.

Helsinki University of Technology
Department of Chemical Technology
Laboratory of Industrial Chemistry

Teknillinen korkeakoulu
Kemian tekniikan osasto
Teknillisen kemian laboratorio

Distribution:
Helsinki University of Technology
Laboratory of Industrial Chemistry
P. O. Box 6100
FIN-02015 HUT
Tel. +358-9-451 2619
Fax. +358-9-451 2622
E-Mail: kanervo@polte.hut.fi

ISBN 951-22-6746-2 (print), 951-22-6747-0 (pdf, available at http://lib.hut.fi/Diss/)
ISSN 1235-6840

Otamedia Oy
Espoo 2003

ABSTRACT

Temperature-programmed desorption (TPD), reduction (TPR) and oxidation (TPO) are thermoanalytical techniques for characterising chemical interactions between gaseous reactants and solid substances. The data collected by these techniques are commonly interpreted on a qualitative basis or by utilising simple, approximate kinetic methods. However, temperature-programmed techniques can also be regarded as transient response techniques and the experimental data can be utilised for dynamic modelling. This work comprises case studies on kinetic analysis of TPR, TPD and TPO related to the characterisation of heterogeneous catalysts. The emphasis is on methodological aspects and on assessing the potential of temperature-programmed data as a source of kinetic information.

Kinetic analysis was applied to the TPR results for series of alumina-supported chromium oxide and vanadium oxide catalysts. Hydrogen was used as the reducing agent. Different kinetic models were tested against the experimental data and parameters were estimated. The chromium oxide and vanadium oxide contents of the catalysts were clearly reflected in the reduction behaviour and in the best-fit kinetic models and their parameters. The kinetic results suggested that reduction takes place via a topochemical mechanism, as growing domains, on both supported chromium and supported vanadium oxide catalysts with close to monolayer content.

The interaction of hydrogen with a commercial nickel catalyst was studied in TPD experiments under continuous flow and ambient pressure. A model to account for the heterogeneity in the chemisorption interaction and for the readsorption was formulated and tested against experimental data. The heterogeneity was described by introducing a sufficient number of different adsorption states. The rapid readsorption occurring during TPD was taken into account by describing the intrinsic dynamics of an adsorption state as a quasi-equilibrium adsorption/desorption between the gas phase and the surface. A model with two adsorption states of hydrogen was able to describe the experimental data with physically acceptable parameters in the temperature range of 323–673 K.

The regeneration kinetics of a deactivated cracking catalyst was investigated on the basis of the experimental evolution rates of carbon monoxide and carbon dioxide during TPO. Different kinetic models were tested and kinetic parameters were estimated. A power-law kinetic expression with orders unity and 0.6 for coke and oxygen, respectively, was capable of describing the experimental data.

In each case study, a phenomenological model was established and the kinetic parameters of the model were determined via nonlinear regression analysis in MATLAB® environment. The results demonstrate that common catalyst characterisation data on reduction, desorption and oxidation collected in the temperature-programmed mode can fruitfully be subjected to detailed kinetic analysis. Mechanism and parameter identifiability require diversity in the experimental data, which can be achieved, for example, by applying multiple heating rates in experiments. Kinetic analysis extends the interpretability of temperature-programmed reactions in catalyst characterisation and it is potentially useful for the elucidation of fundamental reaction mechanistic information and establishing kinetic models for engineering applications.

TIIVISTELMÄ

Lämpötilaohjelmoitu desorptio (TPD), pelkistys (TPR), ja hapetus (TPO) kuuluvat termoanalyyttisiin menetelmiin kaasu-kiinteä aine -vuorovaikutusten karakterisoimiseksi. Näillä menetelmillä kerättyä koeaineistoa on perinteisesti tulkittu kvalitatiivisesti tai yksinkertaisten likimääräisten kineettisten menetelmien avulla. Lämpötilaohjelmoituja karakterisointimenetelmiä voidaan kuitenkin pitää transienttikineettisinä menetelminä, joiden koetuloksia voidaan hyödyntää dynaamisessa mallituksessa. Työ koostuu heterogeenisiin katalyytteihin liittyvien lämpötilaohjelmoitujen desorption, pelkistyksen, ja hapetuksen kineettisistä analyyseistä. Painopiste on menetelmällisissä näkökohdissa ja koetulosten kineettisen hyödynnettävyyden arvioinnissa.

TPR-osassa tutkittiin alumiinioksidikantajallisten kromi- ja vanadiinioksidien vetypelkistyksen kinetiikkaa. Erityyppisten kineettisten mallien yhteensopivuutta koetulosten kanssa testattiin ja kineettiset parametrit estimoitiin regressioanalyysillä. Katalyyttien kromi- ja vanadiinioksidipitoisuus olivat ratkaisevia pelkistysreaktiossa, ja tämä myös ilmeni reaktionopeutta parhaiten kuvaavissa malleissa ja niiden parametrien arvoissa. Saadut tulokset viittasivat topokemialliseen pelkistysmekanismiin sekä kromi- että vanadiinioksidikatalyyteillä, joissa katalyyttistä ainetta oli likimain monokerros. Kineettisten tulosten perusteella oksidikerroksen pelkistys etenee tällöin tiettyjen alkukohtien ympärille kasvavina alueina.

Vedyn vuorovaikutusta kaupallisen nikkelikatalyytin kanssa tutkittiin TPD-kokeilla virtaussysteemissä normaalipaineessa. Koetulosten analyysiä varten kehitettiin malli, joka ottaa huomioon heterogeenisuuden kemisorptiovuorovaikutuksessa ja desorboituneen vedyn takaisinadsorption TPD:ssä. Heterogeenisuus kuvattiin tarvittavalla määrällä erityyppisiä adsorptiotiloja. Nopea takaisinadsorptio otettiin huomioon kuvaamalla kunkin adsorptiotilan adsorptio-desorptio -dynamikka kvasitasapainona pinnan ja kaasufaasin välillä. Sovitettaessa mallia koeaineistoon todettiin kahden adsorptiotilan riittävän selittämään havainnot. Estimoidut adsorptioparametrit olivat fysikaalisesti järkevää suuruusluokkaa.

Deaktivoituneen krakkauskatalyytin regeneroinnin kinetiikkaa tutkittiin TPO-koejärjestelyllä hiilidioksidin ja hiilimonoksidin muodostumisnopeuksien mittauksien perusteella. Erityyppisiä kineettisiä malleja testattiin ja niihin liittyvät parametrit kummankin oksidin

muodostukselle estimoitiin. Kertalukumalli, joka oli kertalukua yksi koksin ja kertalukua 0,6 hapen suhteen, kuvasi hyvin koeaineistoa.

Kaikkien tutkittujen lämpötilaohjelmoitujen kaasu-kiinteä aine -reaktioiden tapauksissa muodostettiin ilmiöpohjainen fysikaalis-kemiallinen malli, jonka kineettiset parametrit määritettiin epälineaarisella regressioanalyysillä MATLAB®-ympäristössä. Työ osoittaa, että tavanomaisesti karakterisointitarkoituksissa kerätty koedata lämpötilaohjelmoidusta pelkistyksestä, desorptiosta ja hapetuksesta soveltuu myös kineettisen analyysin perustaksi. Mekanismien ja parametrien identifioituvuus edellyttää monipuolista koeaineistoa, esim. useiden lämmitysnopeuksien käyttöä kokeissa. Lämpötilaohjelmoitujen reaktioiden kineettinen analyysi laajentaa koetulosten tulkittavuutta ja vertailtavuutta heterogeenisten katalyyttien karakterisoinnissa. Lisäksi se soveltuu suotuisissa tapauksissa reaktiomekanismien selvittämiseen ja prosessisuunnittelussa tarvittavan reaktiokinetiikan määrittämiseen.

PREFACE

The practical work for this thesis was carried out in the Laboratory of Industrial Chemistry, Helsinki University of Technology, between April 1998 and December 2002. Funding was provided by the Academy of Finland through the Graduate School in Chemical Engineering (GSCE) and the project Advanced kinetic modelling of hydrogenation reactions. GCSE organised a diversity of courses and seminars that substantially contributed to my post-graduate education. Additional funding was provided by Fortum Oil and Gas Oy.

I am most grateful to my supervisor, Professor Outi Krause for her guidance and encouragement and the overwhelming enthusiasm that she demonstrated towards my work. I also sincerely thank my co-authors for their contributions to the publications and my other colleagues for their advice. The staff of the laboratory provided a congenial and stimulating working atmosphere.

Noora Lylykangas is thanked for carrying out preliminary work in regard to the reduction kinetics, Jorma Hakala for his assistance with library services, and Dr. Kathleen Ahonen for revising the language of this thesis and three publications.

I am greatly indebted to my parents Marjukka and Osmo and my brother Teemu for their love and support and for providing examples of a fearless attitude towards challenges. Finally, I wish to thank Kalle for sharing his sound physical and algorithmic thinking and for being an inspiring companion in science and in life.

Espoo, May 2003

Jaana Kanervo

LIST OF PUBLICATIONS

This thesis is based on the following publications, which are referred to in the text by the corresponding Roman numerals (Appendices I-V):

I. Kanervo, J.M., Krause A.O.I., Kinetic Analysis of Temperature-Programmed Reduction: Behaviour of a CrO_x/Al_2O_3 Catalyst, *J. Phys. Chem. B* **105** (2001) 9778-9784.

II. Kanervo, J.M., Krause A.O.I., Characterisation of supported chromium oxide catalysts by kinetic analysis of H_2-TPR data, *J. Catal.* **207** (2002) 57-65.

III. Kanervo, J.M., Harlin, M. E., Krause A.O.I., Bañares, M. A., Characterisation of supported vanadium oxide catalysts by kinetic analysis of H_2-TPR data, *Catal. Today* **78** (2003) 171-180.

IV. Kanervo, J. M., Reinikainen, K. M., Krause, A.O.I., Kinetic analysis of temperature-programmed desorption, *Appl. Catal*, A, in press.

V. Kanervo, J.M., Krause A.O.I., Aittamaa, J.R., Hagelberg, P., Lipiäinen, K.J.T., Eilos, I. H., Hiltunen, J.S., Niemi, V.M., Kinetics of the regeneration of a cracking catalyst derived from TPO measurements, *Chem. Eng. Sci.* **56** (2001) 1221-1227.

Jaana Kanervo's contribution to the appended publications is as follows:

I. She set up procedures for model-fitting based parameter estimation for kinetic analysis of TPR data, investigated the description of the kinetics of reactions occurring via the nucleation and nuclei growth mechanism, carried out the kinetic analysis of the reduction of chromium oxide catalyst and wrote the manuscript.

II. She treated the experimental TPR data, carried out the kinetic analysis using nonlinear regression analysis, interpreted the results and wrote the manuscript.

III. She planned and performed the TPR experiments and conducted the kinetic analysis. She contributed to the interpretation of the results and wrote the manuscript together with the co-authors.

IV. She contributed to the design of experiments, developed a model for kinetic analysis of the TPD data, implemented and conducted the nonlinear regression analysis. She interpreted the results and wrote the major part of the manuscript.

V. She conducted the kinetic analysis of the experimental TPO results and implemented the parameter estimation. She interpreted the results and wrote the manuscript with the co-authors.

KINETIC ANALYSIS OF TEMPERATURE-PROGRAMMED REACTIONS

ABSTRACT 1

TIIVISTELMÄ 3

PREFACE 5

LIST OF PUBLICATIONS 6

1 INTRODUCTION 10

1.1 Heterogeneous catalysis and chemical kinetics 10

1.2 Transient kinetics 11

1.3 Analysis of reaction systems under a temperature program 13

Thermoanalytical techniques 13

Temperature-programmed reaction techniques 14

1.4 Kinetic analysis of temperature-programmed reactions 17

Isoconversional methods 19

Methods based on model fitting 21

1.5 Scope of the work 23

2 KINETIC ANALYSIS OF TPR 25

2.1 Temperature-programmed reduction and kinetic analysis 25

2.2 Results and discussion 27

2.2.1 Reaction mechanism of nucleation and nuclei growth 27

2.2.2 Kinetics of the reduction of chromium and vanadium oxide catalysts 29

Experimental results and investigation of kinetics 29

Interpretation of the kinetic results 34

Activation energies of reduction 35

2.3 Conclusions 38

3 KINETIC ANALYSIS OF TPD 39
3.1 Temperature-programmed desorption and kinetic analysis 39
3.2 Results and discussion 42
3.2.1 Experimental results 42
3.2.2 Kinetic models for TPD 43
Validation and testing 45
3.2.3 Pulse chemisorption 48
3.3 Conclusions 49

4 KINETIC ANALYSIS OF TPO 50
4.1 Kinetic analysis of coke combustion 50
4.2 Results and discussion 52
4.3 Conclusions 58

5 ASSESSMENT OF KINETIC ANALYSIS OF TEMPERATURE-PROGRAMMED REACTIONS 59
5.1 Level of information obtainable from TPD, TPR and TPO 59
5.2 Challenges in kinetic analysis of TPx data 60
5.3 Methodological remarks 61
Isoconversional and model-free methods 61
Methods of kinetic analysis based on model fitting and mechanism and parameter identifiability 65

6 CONCLUDING REMARKS 67

7 REFERENCES 68

APPENDICES
Publications I-V

1 INTRODUCTION

1.1 Heterogeneous catalysis and chemical kinetics

Catalysis plays a pivotal role in the physical and biological sciences, in the industrial production of chemicals, 90% of which are obtained via catalytic conversions [1]. Catalysis research covers both multidisciplinary science and engineering.

Catalysis is a kinetic phenomenon and understanding the rates of the chemical steps in catalysis presents a profound challenge to chemists and engineers. The goal of kinetic investigations is to find a model that describes the rate of reaction as a function of state variables that define the chemical process. Chemical kinetics is investigated 1) to obtain fundamental insight into reaction mechanisms, 2) to assist catalyst design and 3) to aid reactor design, process development and optimisation.

At present kinetic analysis of heterogeneous catalytic reactions mainly means fitting models to experimental data involving bulk concentrations of reactants and/or products. The required experiments are carried out in ideal laboratory reactors with as minimal mass and heat transfer limitations as possible. The reaction rate data are typically collected under well-defined steady-state conditions. The kinetic models are of either empirical or mechanistic nature. A fully mechanistic model is established on the basis of elementary steps comprising the adsorption of reactants from the fluid phase to the catalyst surface, the reactions occurring on the surface and the desorption of products from the surface to the fluid phase. Rate equations for parameter estimation are formulated with the aid of rate-determining steps (RDS) and pseudo-steady-state assumptions. Complications may arise, however, in applying the steady-state approach to kinetic analysis. A rate measured under steady state provides information on the convoluted combination of elementary step reactivities. The observable behaviour of a chemical system under steady state can often be explained by more than one mechanistic pathway, which leads to difficult discrimination among rival kinetic models. Thus, conventional kinetic analysis is not always sensitive to the underlying reaction mechanism; it provides lumped kinetic parameters and does not provide predictions of the behaviour of the catalytic system under dynamically changing, i.e. transient conditions.

Transient response methods offer several advantages for investigation of the kinetics of heterogeneous catalytic reactions. Instead of the reaction system being driven to a steady state, the system is perturbed in a controlled way. In principle, any system variable concentration, temperature, flow rate or pressure can be changed. The kinetic experiment can be designed to probe the physico-chemical system (a test reactor containing the catalyst) by appropriate dynamic inputs. The response of the system to the dynamic input is then measured and subjected to kinetic analysis. The most common perturbations for heterogeneous gas-phase reactions are concentration perturbations (concentration steps, pulses or forced periodic concentration oscillations) and temperature perturbations (temperature programming). While undergoing a dynamic change the system reveals more about the intrinsic mechanism: Reaction steps in the series do not necessarily proceed at the same rate and reactive intermediates may accumulate. Ideally, transient experiments allow interpretation of the response in terms of all elementary reactions, and the obtained model is capable of reliable dynamic predictions. The transient response techniques applied to heterogeneous catalysis have been reviewed by Kobayashi and Kobayashi [2], Furusawa et al. [3], Bennett [4, 5], Tamaru [6], Mirodatos [19] and Mills and Lerou [7]. Enlightening modelling and simulation studies on aspects of transient kinetics have been published by Kobayashi [8], Müller and Hofmann [9], Salmi [10], Renken [11], Pekar and Koubek [12,13] and Belohlav and Zamotsny [14,15].

The transient response methods in chemical kinetics place similar requirements on the experimental set-up to conventional methods of kinetic analysis, and some additional ones as well. The mass balances of the reactor should be well described by mathematical models and the mass and energy transfer limitations should be negligible or sufficiently modelled. Criteria for negligible inter- and intra-particle mass and heat transfer limitations have been designed specially for transient experimentation [16]. On-line monitoring of the reactor outlet with sufficient time resolution is necessary for transient kinetic analysis. In addition, the required time behaviour of the dynamic input and the sampling frequency of the output depend on the characteristic dynamics of the studied reaction system. If the dynamics of the transient input is too slow, all or part of the elementary reactions may proceed in quasi-equilibrium. Individual rates of elementary reactions cannot then be properly elucidated.

Sometimes to fully exploit the potential of transient methods and to assess the rates of rapid elementary reactions, a sub-millisecond time resolution may be needed. The Temporal Analysis of Products (TAP) technique makes this possible [17]. In TAP a very narrow pulse of reactant is injected to a reactor system, which is evacuated at the other end. The mass transport takes place in the Knudsen diffusion regime and the output pulse reflects the mass transport and intrinsic reaction kinetics. The disadvantages of TAP are the costly equipment, challenging modelling of all mass transport phenomena in the reactor system and the pressure gap with respect to practical process conditions.

Another special transient response technique is Steady State Transient Kinetic Analysis (SSITKA) [18, 19]. In SSITKA the system is first run to a steady state and then one of the reactants is abruptly changed to an isotopically labelled compound. The rate of exchange of the normal to labelled product compounds, monitored by mass spectrometry, reveals the intrinsic reaction kinetics. The thermodynamic state of the system remains essentially constant in experiments for SSITKA, and the reaction kinetics may be assessed close to a selected steady state. In SSITKA the effect of possible surface reactivity distribution is thus minimised.

The kinetic analysis of transient response data is based on nonlinear regression analysis, which usually is more demanding than nonlinear regression analysis for steady state kinetic analysis. Pseudo-steady state and RDS assumptions are omitted. Dynamic continuity equations are established for each and every gas phase and surface species, which results in a set of coupled differential or partial differential equations [20]. Figure 1.1 presents a general computational scheme for nonlinear regression analysis.

The transient response methods represent advanced kinetic analysis of heterogeneous catalytic reactions. Nevertheless, these methods are presently based on model fitting to experimental data of bulk concentrations, whereas the surface concentrations in catalytic reactions are typically unobservable quantities. Kinetic analysis based on bulk concentrations alone cannot conclusively verify a reaction mechanism. In the future, kinetic analysis can be expected to rely more on spectroscopic in-situ determinations with atomic resolution and on theoretical calculation of the rate constants of elementary steps [21, 22, 23].

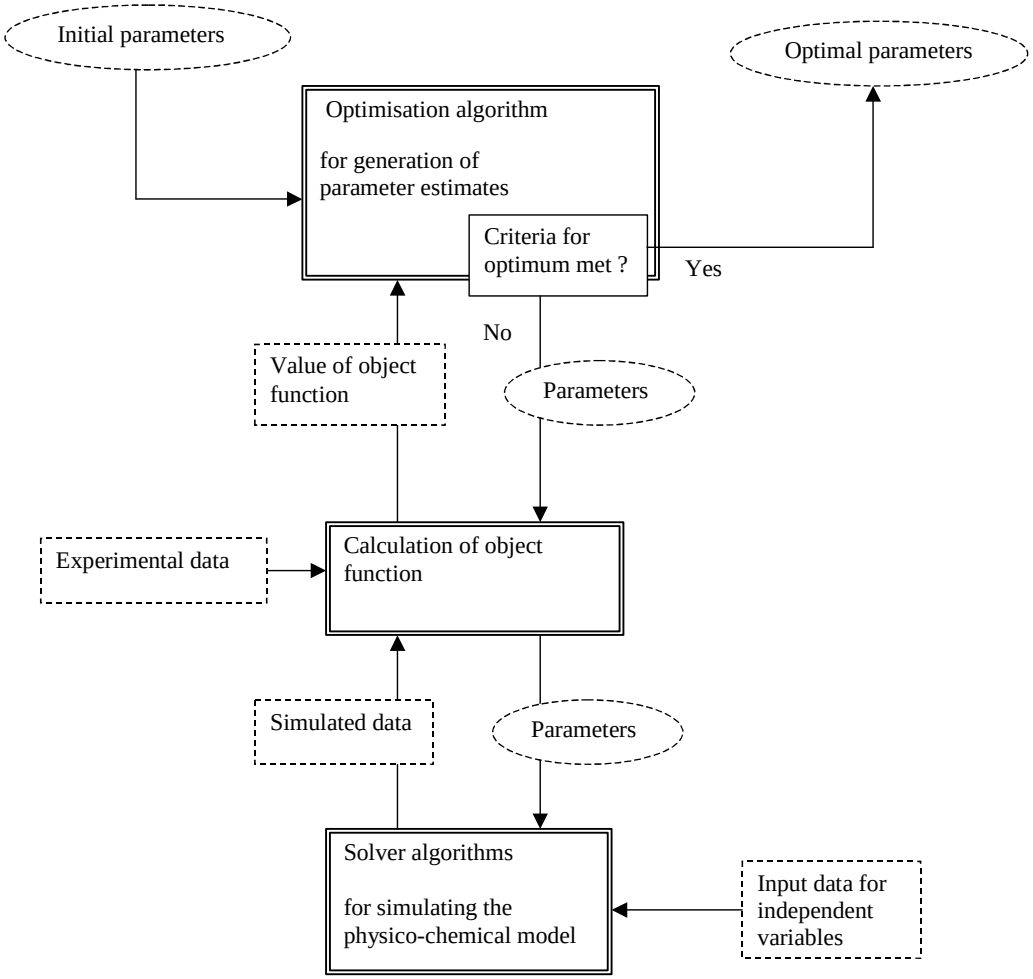

Figure 1.1. Elements of kinetic analysis by nonlinear regression.

1.3 Analysis of reaction systems under a temperature program

Thermoanalytical techniques

Thermoanalytical techniques can be considered as transient response techniques, in which some characteristic property of a solid sample is related to its temperature in a process of programmed heating. Exchanges of matter and/or energy between the sample and its surroundings provide means to detect and follow physical or chemical transformations. The measured response as a function of temperature, the thermogram, reflects the nature of the system under study and the experimental conditions. Thermal analysis is used as a tool for quantitative and qualitative analysis for evaluating the influence of different factors on the reactivity. The most common thermoanalytical techniques are summarised in Table 1.1. A number of methods exist to extract the kinetics of the occurring chemical reactions from thermoanalytical data. An extensive review of the study of heterogeneous processes by thermal analysis, including kinetics and mechanisms of non-catalytic reactions, has been

published by Sestak et al. [24]. In the field of heterogeneous catalysis, thermal analysis is used as tool for investigating the influence of composition, preparation method and pre-treatment on the reactivity of the surface or bulk with gases.

Table 1.1. Thermal analysis techniques.

Abbrev.	Name	Characteristic factor monitored
DTA, DSC	Differential thermal analysis Differential scanning calorimetry	Temperature difference between sample and reference
TG	Thermogravimetry	Weight of sample
DTG	Differential thermogravimetry	Rate of weight changes
TMA	Thermomechanical analysis, Dilatometry	Specific volume of solid sample
TMA	Thermomagnetic analysis	Magnetic susceptibility
DMC	Differential microcalorimetry	Enthalpy difference between sample and reference
TPx	Temperature-programmed reaction (x = Reduction, Oxidation, Desorption, Sulphidation or Surface Reaction)	Gas composition at the reactor outlet

Temperature-programmed reaction techniques

Although thermal analysis is most frequently applied to the decomposition of solid materials, it also constitutes a suitable methodology to assess the kinetics of other thermally stimulated processes. Among the thermoanalytical techniques, temperature-programmed desorption (TPD) and temperature-programmed reduction (TPR) are the most commonly used tools for characterising heterogeneous catalysts. TPD was reported by Amonomiya and Cvetanovic [25] in 1963 and effectively was an extension to powdered solids of the flash desorption technique (developed by Redhead [26]) for the study of the desorption of gases from heated metallic filaments in high vacuum. In TPD studies a solid previously equilibrated with an adsorbing gas is submitted to a programmed temperature rise and the amount of desorbing gas is continuously monitored. TPR was inspired by the TPD technique and proposed in its present form by Robertson et al. [27] in 1975. In TPR the oxidic catalyst precursor is submitted to a programmed temperature rise under a flow of reducing gas mixture and the consumption of the reducing agent is continuously monitored. The temperature-programmed techniques have also been extended to cover oxidation, sulphidation, methanation, hydrogenation, gasification, carburisation and other catalytic surface reactions

(TPO, TPS, TPM, TPH, TPG, TPC, and TPSR, respectively). Alongside catalyst characterisation, temperature-programmed (TPx) techniques can be applied to mimic pre-treatment procedures related to the operation of catalytic processes [28]. The types of information obtainable from the most common TPx techniques are summarised in Table 1.2.

The application of TPD, TPR and related techniques was reviewed by Cvetanovic and Amenomiya in 1972 [29] and by Falconer and Schwarz [30] in 1983, Hurst et al. [31] in 1982 (TPR), Lemaitre [32] in 1984 (TPR), and Jones and McNicol [33] in 1986 (TPR). Bhatia et al. [34] reviewed several temperature-programmed analysis methods and their applications in catalytic systems, covering the years 1983-1990. Their review contains information on the experimental techniques, the theoretical aspects of the analysis and a wide selection of TPx case studies.

Table 1.2. Types of information obtainable from TPx techniques.

TPD, Temperature-programmed desorption
• Characterisation of adsorptive properties of materials • Characterisation of surface acidity • Temperature range of adsorbate release, temperatures of rate maxima • Total desorbed amount, adsorption capacity, metal surface area and dispersion • Surface energetic heterogeneity, binding states and energies of adsorbed molecules • Mechanism and kinetics of adsorption and desorption
TPR, Temperature-programmed reduction
• Characterisation of redox properties of materials, 'fingerprint' of sample • Temperature range of consumption of reducing agent, temperatures of rate maxima • Total consumption of reducing agent, valence states of metal atoms in zeolites and metal oxides • Interaction between metal oxide and support • Indication of alloy formation in bimetallic catalysts • Mechanism and kinetics of reduction
TPO, Temperature-programmed oxidation
• Characterisation of redox properties of metals and metal oxides • Characterisation of coke species in deactivated catalysts • Total coke content in deactivated catalysts • Mechanism and kinetics of oxidation reactions

In TPx techniques a small catalyst sample (typically 10-500 mg) is placed in a reactor system equipped with a programmable furnace. The reactor is a quartz tube fixed bed (i.d. typically 2-6 mm). In TPx runs the pretreated sample is exposed to continuous flow of inert or reactive gas mixture, while the temperature is raised according to a predetermined program. The sample temperature and the outlet gas composition are continuously monitored. Typical detectors for TPx are the thermal conductivity detector (TCD) and mass spectrometer (MS). Use and calibration of the TCD is straightforward, but it is applicable only for binary mixtures of gases. MS provides total monitoring of the outlet gas composition.

Typical experimental conditions [34] applied in TPD, TPR and TPO, together with the experimental conditions used in this work, are listed in Table 1.3. Careful selection of the experimental conditions is essential for novel samples to ensure sufficient detector sensitivity and well-defined mass and heat transfer. Intraparticle diffusion limitations are avoided if possible, the reactor is preferably operated in differential reactor mode and gas-phase reactant exhaustion is prevented. Typically the total pressure and molar flow rate remain practically constant during the TPx run. Experimental configurations have been described for TPD [30], TPR [33] and both together [32]. Figure 1.2 shows the experimental arrangement used in this work (I-IV) [35]. The set-up was a commercial catalyst characterisation system (Zeton Instruments Altamira AMI-100) with a micro catalytic reactor, which is typically operated in differential reactor mode under a well-controlled linear temperature program.

Table 1.3. Typical experimental conditions for TPx [34] and conditions applied in this work.

	TPD	TPR	TPO
Gas composition	He or N_2 or Ar	5% H_2/N_2	5% O_2/N_2
This work	Ar	10% H_2/Ar	0.5-2.0 % O_2/He
Flow rate cm^3/min	15-60	15-30	30-90
This work	30	30-50	30
Heating rate K/min	10-60	4-60	10-60
This work	6-17	6-17	5-10
Detector	TCD or MS	TCD	TCD or MS
This work	TCD	TCD	FID
Measured quantity in this work	H_2 evolved	H_2 consumed	CO, CO_2 evolved

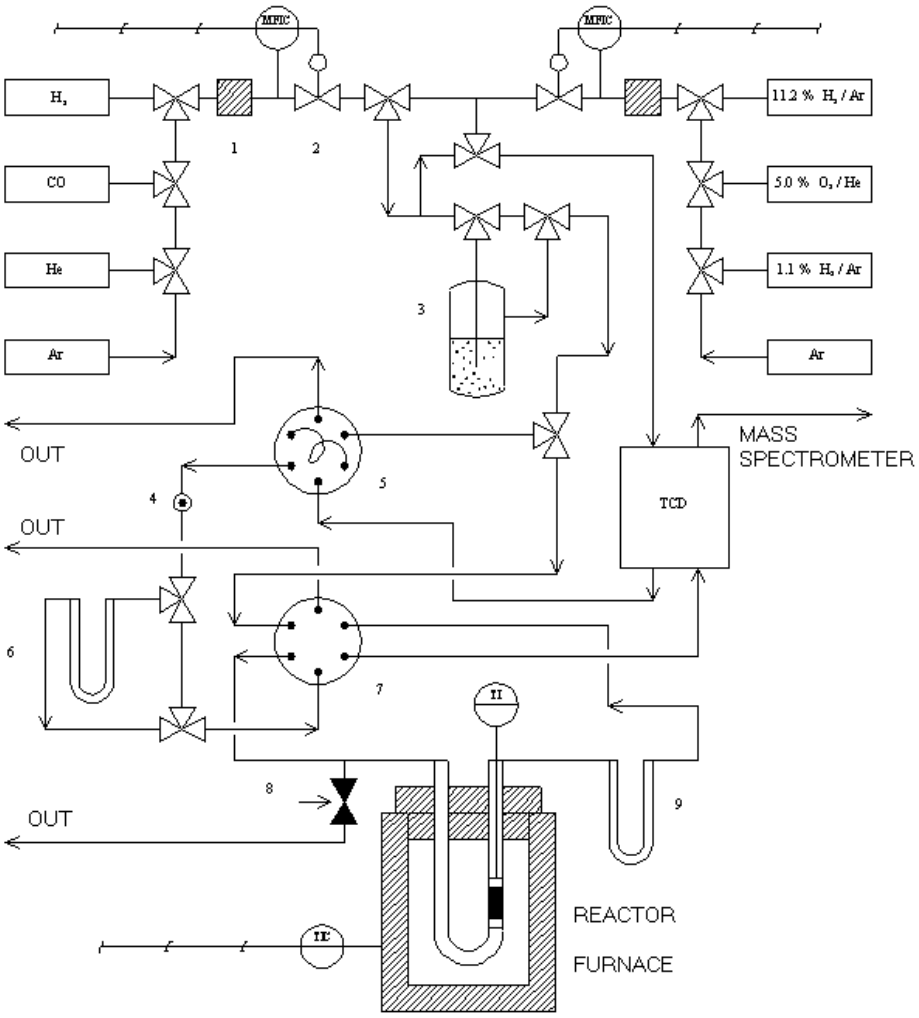

Figure 1.2. TPR/TPD equipment [35]: (1) filter, (2) mass flow controller, (3) gas saturator, (4) injection port, (5) 6-ways-valve with gas dosage, (6) reference reactor, (7) 6-ways-valve, (8) safety valve and (9) trap.

1.4 Kinetic analysis of temperature-programmed reactions

Kinetic analysis for TPx and other thermoanalytical experiments has been carried out by various methods, but it is best established on phenomenological basis. Bhatia et al. [34] list kinetic modelling approaches that have been used for the analysis of TPx experiments. Modelling of TPD data is based on theories on adsorption and desorption, while TPR and TPO call for an understanding of gas–solid reaction mechanisms, which may include topochemical characteristics. In contrast to a homogeneous reaction a topochemical reaction takes place at the interface between solid substrate and solid product. The rate of a topochemical reaction can be divided into two parts: (a) the intrinsic rate of reaction per area of reaction interface and (b) the change in the reaction interface in the course of the reaction [36]. Reduction and oxidation reactions of solids may well exhibit topochemical dynamics, whereas adsorption and desorption on the catalytic surfaces are typically homogeneous

reactions. Despite the differences in intrinsic reaction mechanisms associated with the various TPx techniques, the kinetic analyses largely share the same methodical basis.

Kinetic analysis of thermoanalytical data where there is a linear temperature rise (β) has most often been based on the rate equation

$$\beta \frac{d\alpha}{dT} = A\exp\left(\frac{-E}{RT}\right) f(\alpha), \qquad (1.1)$$

which states that the rate of the reaction is proportional to the rate coefficient with Arrhenius temperature-dependence (A=pre-exponential factor, E=activation energy) and a function of the degree of conversion, $f(\alpha)$. Concentration of a solid is not usually a meaningful term for solid-state reactions. If gaseous reactants or products are involved in the reaction, a function of their concentrations $f_2(C_i)$ is included in eq. 1.1. The functions $f(\alpha)$ and $f_2(C)$ originate from physico-geometric considerations and/or the law of mass action. Table 1.4 collects alternative reaction models $f(\alpha)$ for solid-state kinetics and g(α), i.e. integrals of $1/f(\alpha)$ [37].

Table 1.4. Common physico-geometric kinetic model functions for solid-state reactions [37].

	Model name	f(α)	g(α)
A	Random nucleation, Deceleratory first-order	$(1-\alpha)$	$-\ln(1-\alpha)$
B	Generalised nth order	$(1-\alpha)^n$	$1/n(1-(1-\alpha)^{-(n-1)})$
C	1D or 2D Avrami- Erofeyev	$2(1-\alpha)(-\ln(1-\alpha))^{1/2}$	$(-\ln(1-\alpha))^{1/2}$
D	2D or 3D Avrami- Erofeyev	$3(1-\alpha)(-\ln(1-\alpha))^{2/3}$	$(-\ln(1-\alpha))^{1/3}$
E	3D Avrami- Erofeyev	$4(1-\alpha)(-\ln(1-\alpha))^{3/4}$	$(-\ln(1-\alpha))^{1/4}$
F	Generalised Avrami- Erofeyev	$n(1-\alpha)(-\ln(1-\alpha))^{(n-1)/n}$	$(-\ln(1-\alpha))^{1/n}$
G	Contracting area Sharp interface controlled reaction	$(1-\alpha)^{1/2}$	$2(1-(1-\alpha)^{1/2})$
H	Contracting volume Sharp interface controlled reaction	$(1-\alpha)^{1/3}$	$3(1-(1-\alpha)^{1/3})$
I	Generalised model by Sestak	$\alpha^m(1-\alpha)^n(-\ln(1-\alpha))^p$	
J	Prout-Tompkins model	$\alpha\,(1-\alpha)$	$\ln(\alpha/(1-\alpha))$
K	One-dimensional diffusion	$½\,\alpha$	α^2
L	Two-dimensional diffusion	$-\ln(1-\alpha)-1$	$(1-\alpha)\ln(1-\alpha)+\alpha$
M	Three-dimensional diffusion, Jander	$3(1-\alpha)^{2/3}/(2(1-(1-\alpha)^{1/3}))$	$(1-(1-\alpha)^{1/3})^2$
N	Three-dimensional diffusion, Ginstling-Brounshtein	$3/2((1-\alpha)^{-1/3}-1)$	$(1-(2\alpha/3)-(1-\alpha)^{2/3})$

The Arrhenius-type temperature dependence for homogeneous gas-phase reactions is theoretically based on the Maxwell–Boltzmann energy distribution function. The Arrhenius equation has also been generally accepted and successfully applied to numerous reactions involving solids, but its application is justified by different arguments than those for homogeneous gas-phase system [37, 38].

The application of equation 1.1 is confined to the description of one intrinsic forward reaction or a set of consecutive reactions with one clearly rate-determining step that dominates over the whole range of conditions. The single-step model (eq. 1.1) often appears insufficient to describe the observed transformations. In addition, certain topochemical models cannot be presented in the functional form of eq. 1.1 even though the intrinsic reaction is assumed to take place as a single-step forward reaction. The overall rate process may be of convoluted nature, such as are nucleation and subsequent nuclei growth.

Isoconversional methods

Some simple methods exist for extracting activation energies from thermoanalytical data, assuming that eq. 1.1 provides a sufficient description of the dynamics (condition 1). Kissinger [39] presented one such method for evaluating the activation energy from DTA data. The Kissinger method is based on on eq. 1.1, the second derivative with respect to temperature of which is assigned to zero at the rate maximum:

$$\frac{d}{dT}\left(\frac{d\alpha}{dT}\right)_{T=T_{\max}} = \frac{d}{dT}\left(\frac{A}{\beta}\exp\left(-\frac{E}{RT}\right)f(\alpha)\right)_{T=T_{\max}} = 0 \tag{1.2}$$

$$\Leftrightarrow \quad \left(\frac{A}{\beta}\frac{E}{RT^2}\exp\left(-\frac{E}{RT}\right)f(\alpha)+\frac{A}{\beta}\exp\left(-\frac{E}{RT}\right)\frac{df(\alpha)}{d\alpha}\frac{d\alpha}{dT}\right)_{T=T_{\max}} = 0 \tag{1.3}$$

$$\Leftrightarrow \quad \left(\frac{d\alpha}{dT}\left(\frac{E}{RT^2}+\frac{A}{\beta}\exp\left(-\frac{E}{RT}\right)\frac{df(\alpha)}{d\alpha}\right)\right)_{T=T_{\max}} = 0 \tag{1.4}$$

$$\Leftrightarrow \quad \left(\frac{E}{RT^2}+\frac{A}{\beta}\exp\left(-\frac{E}{RT}\right)\frac{df(\alpha)}{d\alpha}\right)_{T=T_{\max}} = 0 \tag{1.5}$$

$$\Leftrightarrow \quad \frac{E}{RT_{\max}^2} = \frac{A}{\beta}\exp\left(-\frac{E}{RT_{\max}}\right)\left(-\frac{df(\alpha)}{d\alpha}\right)_{T=T_{\max}} \tag{1.6}$$

The Kissinger method relates the temperatures of the rate maxima (T_{max}) obtained with different heating rates (β) to the activation energy (E):

$$\ln\left(\frac{\beta}{T_{\max}^2}\right)+\ln\left(\frac{E}{RA}\right)=-\frac{E}{RT_{\max}}+\ln\left(-\frac{df(\alpha)}{d\alpha}\right)_{T=T_{\max}} \tag{1.7}$$

Thus, if the plot of $ln(\beta/T_{max}^2)$ versus $1/T_{max}$ results in a straight line, the slope of the line equals $-E/R$, provided that the last term of eq. 1.7 is constant (condition 2). Kissinger presented the method for a first-order reaction, but the method is indifferent towards the reaction mechanism $f(\alpha)$ if conditions 1 & 2 are satisfied. Condition 2 is precisely valid for models where $f(\alpha)$ is linear in α (random nucleation model in Table 1.4), but it holds approximately for many models around typical conversion level at the rate maximum ($\alpha \sim 0.6$), as illustrated in Figure 1.3.

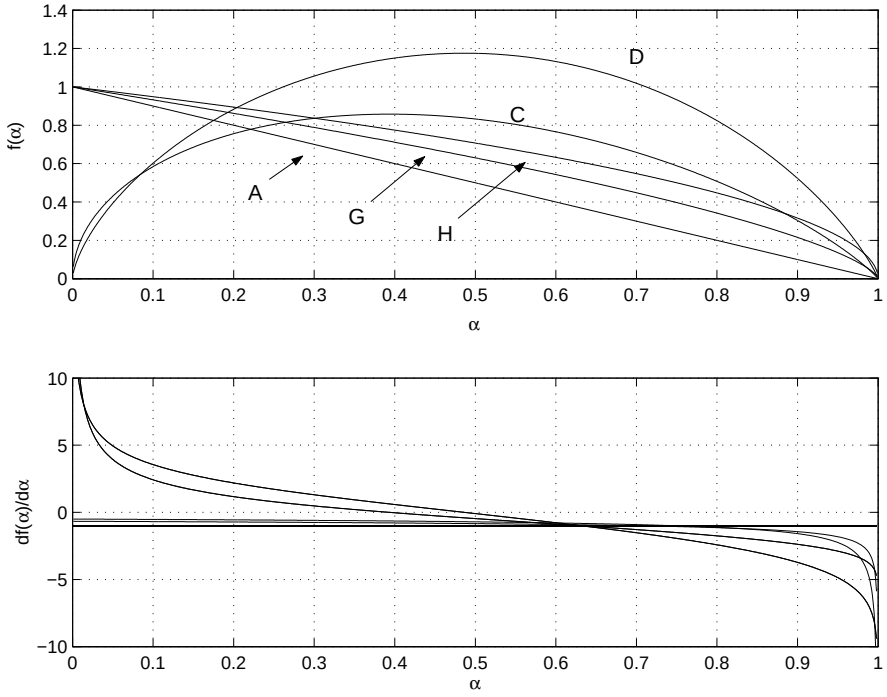

Figure 1.3. Some common functions f(α) and their derivative functions. Letters refer to Table 1.4.

There are other methods, in which the activation energy is calculated at desired degrees of conversion. Friedman [40] introduced the first such method for DTA patterns of polymer degradation. This method is based on transforming eq. 1.1 by taking natural logarithms on both sides of the equation

$$\ln\left(\beta\frac{d\alpha}{dT}\right)=\ln\left(A f(\alpha)\right)-\frac{E}{RT} \tag{1.8}$$

If the plot of $ln(\beta\, d\alpha/dT)$ versus $1/T$ results in a straight line at a selected conversion level, the slope of the line equals $-E/R$ at that conversion level. Again, the Friedman method does not assume more of the reaction mechanism than the functional form of eq. 1.1. On the other

hand, if variable activation energy $E=E(\alpha)$ results from the Friedman analysis, it indicates that no model of the form of eq. 1.1 with a normal physico-chemical interpretation describes the reaction kinetics.

Methods based on model fitting

More general approach exists for kinetic analysis than extraction of activation energy values using the above simple methods. The kinetic analysis of TPx profiles can be performed with the use of model fitting and nonlinear regression analysis. This approach allows testing of alternative reaction mechanisms. Kinetic analysis based on model fitting can be divided into several sub-tasks, such as

- mathematical description of the relevant physico-chemical phenomena,
- establishment of a simulation model incorporating numerical algorithms implemented in a programming language,
- iterative computational determination of optimal parameter estimates,
- evaluation of the goodness of the model and the statistical confidence of the parameters

Typically, in the field of thermal analysis eq. 1.1 is numerically solved for α and the kinetic parameters are adjusted until the model solution fits the experiments. Eq. 1.1 is a separable differential equation and the integral of $1/f(\alpha) = g(\alpha)$ is readily found for common reaction models (Table 1.4). The integral of the rate coefficient with respect to temperature is evaluated with approximate formulas [41] or by using numerical integration.

In TPx experiments, the conversion of the solid is not usually a directly observable quantity, but it needs to be related to the observable consumption of a gaseous reactant or to the evolution of gaseous products. Furthermore, models of type eq. 1.1 for the intrinsic rate may be too limiting. The kinetic analysis of TPx experiments is thus better established on a general methodology of transient kinetics that starts with a consideration of the dynamic balance equations for all the relevant gaseous and solid species. Once the intrinsic rate expressions for solid species have been postulated, the reactor model is selected. Formally, the reactor is a packed bed reactor, which can be modelled as such or applying simpler reactor models: an ideal continuous stirred tank reactor (CSTR) or a differential reactor model. The application of simpler reactor models is often well justified. If the concentration of the gaseous reactant remains practically constant along the reactor in the course of the

reaction and if evolved gaseous products do not influence the intrinsic reaction rates, the dynamic CSTR or differential reactor model is an appropriate choice. Furthermore, if the space-time of reactor is very small, as is often the case with the TPx set-up, there is practically no accumulation of species in the gas phase and the accumulation term can be left out of the balance equation. In this case, the conversion of solid is assumed to follow directly the observed rate of reaction. Typical treatment of TPx data inherently contains the differential reactor assumption with negligible accumulation of species in the gas phase. Examples of transient reactor models (balances) can be found in refs. [4, 5, 9, 10, 20].

Even though the reactor dynamics are often adequately described with the differential reactor model, complicating conditions may arise that do not allow the differential reactor assumption. If the conversion of gaseous reactant is non-negligible, that reactant may require its own dynamic balance equation, which is coupled with the equations of the solid species. Considerable consumption of gaseous reactant induces rate differences and thus concentration gradients along the reactor axis. Another factor inducing concentration gradients along the reactor axis is the occurrence of a backward reaction, the rate of which is a function of the concentration of the gaseous product. These situations, or the occurrence of reactions with multiple rate controlling steps, may require the application of a complete packed bed reactor model. Selection of the correct reactor model depends on the characteristics of the particular physico-chemical system.

After the mathematical description of the physico-chemical system of TPx is complete, a simulation model of the system is implemented with suitable numerical algorithms. The parameter estimation with model fitting to the experimental data is conducted according to the principles of Fig. 1.1 and it is accompanied by sensitivity analysis. Reference textbooks on nonlinear regression analysis have been authored, for example, by Bard (1974) [42], Bates and Watts (1988) [43], Seber and Wild (1989) [44], Walter and Pronzato (1997) [45]. Kinetic analysis of TPx data can be considered as a general task of transient kinetics with iterative testing and rejection or acceptance of mechanistic model hypotheses. Like all successful kinetic modelling, the kinetic modelling of TPx requires experimental data with sufficient information content to allow mechanism and parameter identification.

1.5 Scope of the work

Temperature-programmed techniques are valued for providing catalyst characterisation of a chemical nature, under conditions that do not necessarily differ much from real operating conditions of the catalyst. The interpretation of temperature-programmed reduction, oxidation and desorption spectra is usually confined to a discussion of rate maximum temperatures, the number of more or less resolved peaks or determination of the total consumption of reactant or evolution of product. This work focused on quantitative kinetic analysis of reactions under temperature programming. The objectives were to evaluate, develop and apply methods of kinetic analysis and models for a selection of gas–solid reactions. The work aimed to demonstrate that a moderate number of temperature-programmed experiments, carried out with multi-purpose characterisation equipment, can be utilised to test mechanistic models and to determine kinetic parameters, which together describe the rates of reactions. The thesis comprises the present summary and four published case studies. The case studies deal with the temperature-programmed reduction of alumina-supported chromium oxide (I-II) and vanadium oxide (III) catalysts, the temperature-programmed desorption of hydrogen from an alumina-supported nickel catalyst (IV) and the temperature-programmed oxidation of coke from a deactivated cracking catalyst (V). Kinetic analyses of reduction and desorption can serve as tools for assisted catalyst design, whereas kinetic modelling of the regeneration is of interest for process engineering.

Understanding reduction behaviour is essential for catalyst development. In many cases it is the reduction treatment that creates the active sites of catalyst. Studies on kinetics of reduction can aid the selection of pre-treatment conditions for oxidic catalyst precursors and aid the understanding of reactions occurring via redox mechanism. In addition, kinetic modelling of reduction provides, in favourable cases, fundamental information on the underlying gas–solid reaction mechanisms.

Kinetic models for catalysed reactions typically contain a large number of parameters. Thus a separate determination of adsorption and desorption kinetics and energetics of participating species would be welcome. Kinetic analysis of temperature-programmed desorption (TPD) spectra was applied to obtain information on these phenomena. Understanding of hydrogen adsorption on the metal catalyst is expected to benefit the understanding of hydrogen transfer

reactions on this catalyst. In addition, temperature-programmed desorption may provide a means to quantitatively characterise possible surface energetic heterogeneity.

An understanding of regeneration kinetics is required for the development of an optimal catalyst regeneration unit in which the catalyst activity can be restored in a controlled manner. Since the regenerator often produces the heat required for the endothermic catalytic process, the kinetics of regeneration is intricately involved in the mass and energy balances of the coupled process unit. The case study on temperature-programmed oxidation was included in the work to assess the suitability of TPO for elucidating the kinetics of coke oxidation. The methodical foundation is the same as that for the other temperature-programmed techniques.

The following chapters 2–4 summarise the main findings of publications I–V. Characteristics of the kinetic analysis of temperature-programmed gas–solid reactions are discussed in chapter 5.

2 KINETIC ANALYSIS OF TPR

2.1 Temperature-programmed reduction and kinetic analysis

Temperature-programmed reduction (TPR), proposed in its present flow set-up by Robertson et al. [27] in 1975, is one of the most important techniques for catalyst characterisation. The catalytic material on a support is commonly present after preparation as oxidic precursors and the catalyst is activated by reductive pre-treatment. TPR provides essential information on the reducibility of these oxidic precursors. Reducibility is also of key importance for catalysts working via Mars–van Krevelen redox mechanism [46], in which the oxidation of the hydrocarbons proceeds by reduction of an oxidised surface site, which is subsequently re-oxidised by gas-phase molecular oxygen. The average oxidation state during the catalytic operation depends on the relative rates of the reduction and reoxidation. For catalysts working via redox mechanism, TPR consequently characterises one aspect of the catalytic activity.

The TPR experiment results in the consumption of the reducing agent as a function of temperature, generally termed a 'thermogram'. Theory and applications of the TPR technique have been comprehensively reviewed by Hurst et al. [31], Jones and McNicol [33], Lemaitre [32], Bhatia at al. [34] and Knözinger [47]. TPR has been applied to study the influence of support materials, preparation and pre-treatment procedures, and the influence of additives on the reduction behaviour of a catalytic material. TPR also reveals possible alloy formation in bi-metallic catalysts. TPR provides a fingerprint of the redox properties of a catalyst, which can be compared with reference thermograms, and it provides the total consumption of the reducing agent, which can be correlated with the change in the valence state of the reducible substance. Multiple reduction rate maxima appearing in a thermogram are commonly attributed to complexity in the underlying chemical reactions: to occurrence of a multi-step reduction mechanism or to multiple reducing species. Alongside this conventional interpretation of thermograms, the results of well-controlled TPR experiments can be regarded as a source of kinetic data on reduction.

Methods to extract activation energies with the use of other thermoanalytical techniques (DTA, TPD, etc.) have been adapted to TPR studies. The Kissinger [39] and Friedman [40] methods were introduced to TPR studies by Wimmers et al. [48] and Tarfaoui [49],

respectively. The kinetic analysis of TPR data based model fitting allows more profound characterisation of the reduction process than the above-mentioned methods, since reaction mechanisms can be tested while estimating the kinetic parameters, and the data in thermograms are utilised completely. In early work, parameter estimation by model fitting applied first-order rate expressions with a differential reactor model [50,51,52]. The selection of experimental conditions, parametric sensitivity and estimation of kinetic parameters have been dealt with by Monti and Baiker [50] and Malet and Caballero [51], who aided in establishing the quantitative basis of the TPR technique. Wimmers et al. [48] have suggested the utilisation of a wider set of gas–solid reaction mechanisms. Tarfaoui [49] review models for describing kinetics of gas–solid reactions and report case studies on the kinetic analysis of reduction of copper oxide, manganese oxides and alumina-supported vanadium oxide. Despite the widespread use of TPR for catalyst characterisation, kinetic modelling of TPR data has attracted relatively little attention.

In this work, kinetic modelling of TPR data was applied to elucidate the reduction kinetics of supported chromium and vanadium oxide catalysts (I, III). The main method in the kinetic analysis was nonlinear regression analysis. The TPR studies on supported vanadia catalysts were supplemented by X-ray diffraction (XRD) and Raman spectroscopy (III) investigations. Chromium and vanadium oxides are important catalytic materials. Chromium oxide catalysts are applied in polymerisation, hydrogenation/dehydrogenation, oxidation, isomerisation, aromatisation and deNO_x reactions [53], while supported vanadium oxides catalyse selectively numerous partial oxidation reactions, oxidative dehydrogenation and deNO_x reactions [54]. Both oxide systems have been extensively investigated previously. Vanadium oxide catalysts have been characterised, for example, by IR and Raman spectroscopy, UV-VIS DRS, XPS, ESR, XRD, XANES/EXAFS, solid state ^{51}V NMR, TPR, TPO, chemisorption and isotopic labelling [54]. There remain unanswered questions related to the factors influencing the catalytic activity and the structure of active sites in different environments.

The following sections summarise the main findings of publications I-III. First the characteristics of a nucleation and nuclei growth reduction model (I) that proved useful in the interpretation of reduction kinetics of supported oxide catalysts are reviewed. Then the main results of TPR case studies involving chromium and vanadium oxide catalysts (II, III) are presented and discussed.

2.2 Results and discussion

2.2.1 Reaction mechanism of nucleation and nuclei growth

Nucleation and nuclei growth (N/NG) mechanisms are an important class of reaction mechanisms for gas–solid and solid-state reactions. Nucleation occurs as a transformation is initiated at specific locations (so-called germ nuclei) in an old phase and is followed by the growth of nuclei, i.e. domains of new phase, in the surroundings of the starting points. The transformation is complete when the growing domains of the new phase reach the boundaries of the converting material and the boundaries of one another. Together these dynamic processes determine the macroscopically observable conversion–time behaviour. Various phase transformations such as crystallisation, polymerisation and decomposition take place as N/NG processes.

Rates of reactions occurring via N/NG mechanisms can be described in various ways. A well-known approach within gas–solid and solid-state reaction kinetics to account for N/NG behaviour is the Avrami–Erofeyev model, which in other contexts is called the Johnson–Mehl–Avrami–Kolmogorov model. Modifications of the model (derived by Avrami in 1939–1941 [55,56,57]) are widely applied to regress kinetic data of various transformations, and papers on the theoretical aspects are still being published [58,59,60].

In the following the most important characteristics of Avrami kinetics are summarised and interpreted for a system where the transformation is driven by a chemical reaction. The converted volume at time t is given by

$$V_{ex}(t) = \int_0^t v(t,y) \left(\frac{dN}{dt}\right)_{t=y} dy \tag{2.1}$$

where the elements are

a law of nucleation: $\left(\frac{dN}{dt}\right)_{t=y}$ (2.2)

a law of nuclei growth: $v(t,y,)$ (2.3)

and N denotes the number of active (growing) nuclei and $v(t,y)$ gives the volume at time t for a nucleus that became activated at time y. A nucleus radius grows proportionately to a rate constant and the nuclei volume is expressed as a function of the rate constant. For

conversions of chemical nature, the rate constant can be assigned the Arrhenius temperature dependence with the parameters A_g and E_g:

$$v(t,y) = K_g\left(\int_y^t A_g \exp\left(-\frac{E_g}{R(\beta\tau + T_0)}\right)d\tau\right)^m \qquad (2.4)$$

Other parameters are m, the dimensionality of nuclei growth and K_g, the shape factor. Here temperature is assumed to rise as a linear function of time: $T = T_0 + \beta t$

The law of nucleation is commonly described as the first-order decay of germ nuclei (N_0):

$$\frac{dN}{dt} = k_2(t)(N_0 - N) \qquad \Leftrightarrow \qquad \left(\frac{dN}{dt}\right)_{t=y} = k_2(y)\,N_0 \exp(-\int_0^y k_2(t^*)dt^*) \qquad (2.5)$$

Again the rate coefficient k_2 is temperature dependent according to the Arrhenius law.

The application of eqs. (2.4) and (2.5) to (2.1) completes the description of conversion by extended (unlimited) growth of nuclei. The actual volume (V) is extracted from the extended volume (V_{ex}) by the relation given by Avrami [55,56]:

$$V_{ex} = -\ln(1-V) \qquad (2.6)$$

The formulation of eq. (2.6) originates from statistical considerations. It is only approximate, however, and requires, among other things, a random distribution of germ nuclei.

The convolution integral (2.1) can be analytically solved (for example, by using Laplace transformation) for isothermal and so-called isokinetic phase transformations. Commonly, the conversion as a function of time, obtained as the exact solution of (2.1.) combined with (2.6.), is further simplified to various limiting cases that are customarily used in applications. These simplifications may be easily abandoned (I).

The nucleation and nuclei growth model for two-dimensional transformation appeared promising for the reduction of supported chromium oxide. For that reason the foundations of the model were investigated in publication I, and an equation for a more general non-isothermal chemical transformation was formulated.

2.2.2 Kinetics of the reduction of chromium and vanadium oxide catalysts

Experimental results and investigation of the kinetics

Reduction of six chromia and three vanadia catalysts with hydrogen was investigated by H_2-TPR (I-III). Table 2.1 lists the studied catalysts. The chromia catalysts labelled with 'ALD' were prepared by atomic layer deposition (ALD) gas-phase technique, and a commercial fluidised bed chromia catalyst 'FB' was included in the studies as a reference. Vanadium oxide catalysts (V2, V5 and V11) were prepared by incipient wetness impregnation. Approximately 10% hydrogen in argon was used as reducing agent in the TPR experiments. Experimental details can be found in publications II and III.

Table 2.1. Catalyst samples investigated by TPR (I-III).

Sample		Cr or V wt-%	Cr or V atoms/ nm^2 support	AOS*
CrO_x/Al_2O_3	ALD1	1.2	0.7	+2.6
	ALD2	4.7	2.9	+2.7
	ALD3	7.5	4.6	+2.9
	ALD4	11.9	7.3	+2.8
	ALD5	13.5	8.2	+2.5
	FB	12-14	-	+2.5
VO_x/Al_2O_3	V2	2.0	1.4	+4.0
	V5	5.2	3.7	+3.7
	V11	11.4	9.4	+3.6

* AOS = average oxidation state after reduction based on total hydrogen consumption assuming initial valence states Cr^{6+} and V^{5+}.

Results of TPR experiments with the chromium (ALD1-ALD5) and vanadium (V2, V5 and V11) oxide catalysts are presented in Figure 2.1. All chromium oxide catalysts and the vanadium oxide catalyst V2 produced a single-peak TPR pattern. The vanadium oxide catalyst V11 produced two peaks and clearly reduced at two separate stages, and the vanadium oxide catalyst V5 produced a single but broadened TPR peak. The average oxidation states of chromium and vanadium after the reduction, calculated from total hydrogen consumption, are listed in Table 2.1. The chromium appeared to reduce predominantly from Cr^{6+} to Cr^{3+} or Cr^{2+}, and the vanadium from V^{5+} to V^{4+} or V^{3+}.

For chromium oxide catalysts the reduction process shifted to lower temperatures with increasing chromium loading (See Fig. 2.1. a). For samples ALD2–ALD5 the shape of the

TPR pattern was preserved with increasing loading, but for ALD1 the TPR pattern was distinctly different. Increased loading also shifted the reduction of supported vanadium oxide surface species to lower temperature (Fig 2.1. b). The shift was more evident in the TPR patterns reported by Stobbe-Kreemers at al. [61], which clearly showed the temperature of maximum reduction rate to decrease as a function of vanadium oxide coverage on alumina (1.0 – 3.1 V/nm^2) and respectively by Blasco et al. [62] (1.2 – 4.4 V/nm^2). Application of XRD (III, Figure 2) at different temperatures conclusively demonstrated a relationship between the high-temperature reduction process of V11 and the reduction of crystalline $AlVO_4$.

The increase in the reduction rates of supported vanadium and chromium oxides with loading has commonly been attributed to the increase in the degree of polymerisation [53, 54]: isolated monomeric surface oxide species on alumina are assumed to reduce more slowly than polymeric species. It is noteworthy that, for titania-supported vanadia catalysts, the reduction rates of the monomeric and polymeric species are reversed, as was recently found by Bulushev et al. [63]. Evidently, the reduction behaviour depends notably on the support material.

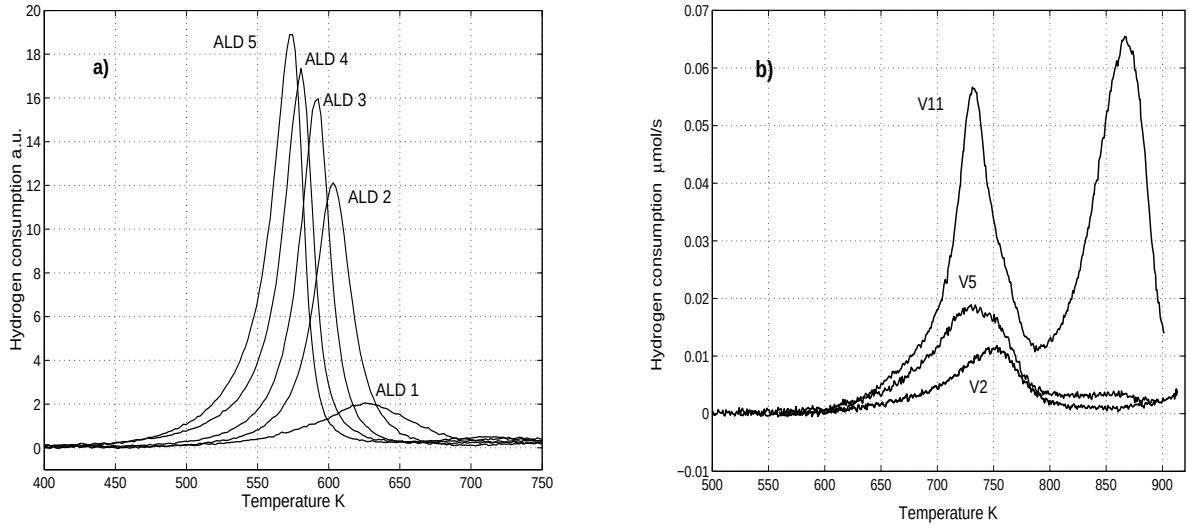

Figure 2.1. TPR patterns of the a) CrO_x/Al_2O_3 and b) VO_x/Al_2O_3 catalysts.

Figure 2.2 shows the temperature-programmed (TP) Raman spectroscopy results for the sample V5. There is a clear gradual decrease in the Raman bands for V=O and V-O-V stretching modes with temperature. The Raman spectroscopy results (III) indicated the

presence of both monomeric and polymeric surface vanadium oxide species on the catalysts V2 and V5, but the ratio of polymeric to isolated species was higher on V5 than V2. For the catalyst V11, intense Raman bands for $AlVO_4$ emerged in the spectra (III, Figure 4).

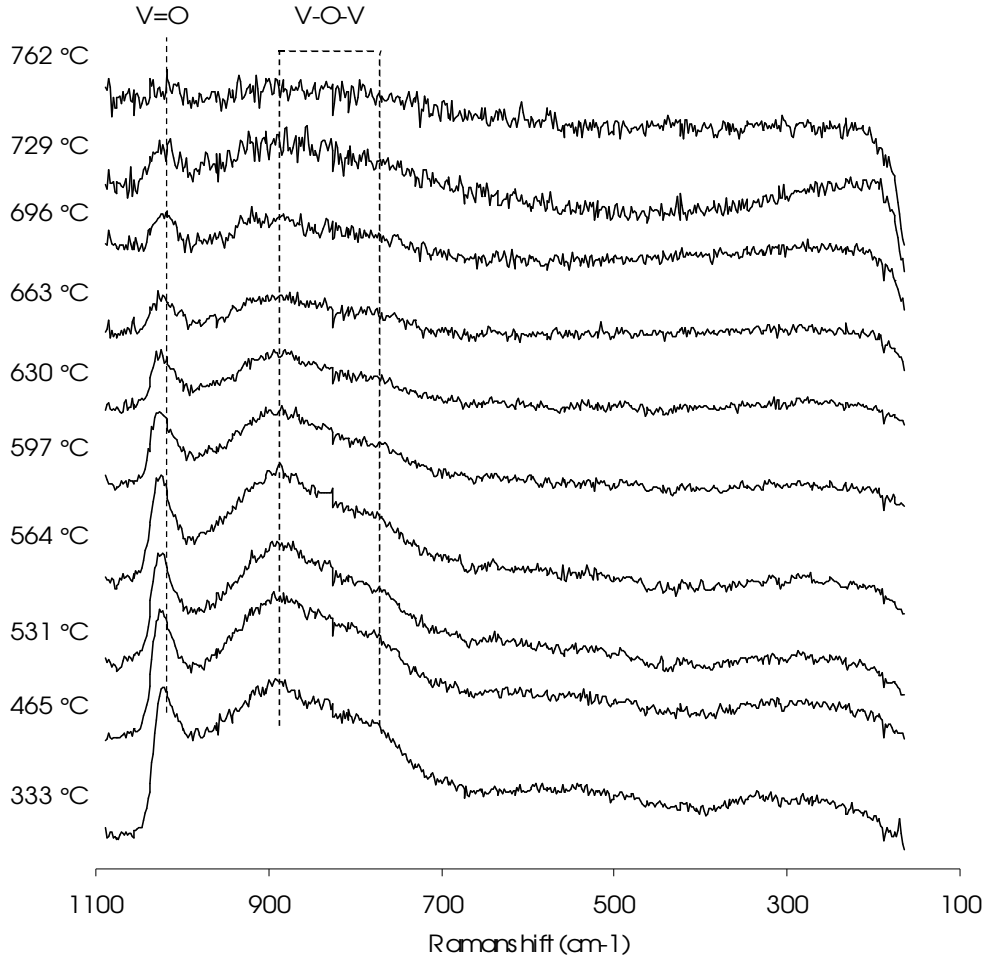

Figure 2.2. TP-Raman spectra of the catalyst V5 under hydrogen.

The Kissinger and Friedman methods were applied to extract the apparent activation energies of reduction for the chromium oxide catalysts (II). The Friedman analysis for ALD3, ALD4, ALD5 and FB gave an approximately constant apparent activation energy up to a reduction degree of 0.5 and a slightly rising trend from there on (II). This implies that, despite the well-controlled preparation and ideal TPR patterns of chromia catalysts, the reduction involved some heterogeneous features. The TPR patterns of the vanadium oxide catalysts (III) were too non-ideal for use of the Kissinger and Friedman methods. Tarfaoui [49] nevertheless applied Friedman analysis to TPR data of an alumina-supported vanadia catalyst (3.11 V/nm^2) and reports three regions of activation energies as a function of degree of reduction. Again this reveals the composite nature of apparently single peak reduction data.

The primary kinetic analysis was carried out with the use of model-fitting based nonlinear regression analysis in MATLAB® 6 environment. The measured hydrogen consumption was directly related to the rate of reduction; consequently the treatment inherently involved the differential reactor assumption. The observed rates of reduction were several orders of magnitude slower than the diffusion rates of gases in the catalyst pores, which means that rates of reduction were kinetically controlled. In addition, the maximum instantaneous conversion of hydrogen was less than 7 %, so that the partial pressure of hydrogen was virtually constant during the whole reaction. The formed water was assumed to have a negligible effect on the observed rate of reaction owing to the low H_2O concentration. Various gas–solid reaction models were tested for the TPR experiments.

As is commonly the case, several models could be fitted to the single scan TPR data of the chromia catalysts. Model discrimination required simultaneous use of experimental data obtained at different heating rates. Three heating rates were sufficient to discriminate kinetic models. The TPR data of each chromium oxide catalyst were described by a single reduction process, whereas the TPR data of the samples V5 and V11 required interpretation in terms of multiple processes. The best-fit kinetic models for the reduction of the chromium oxide catalysts are reported in Table 2.2 and those for the vanadium oxide catalysts in Table 2.3. Figure 2.3 shows the best-fit model solutions and the experimental data of the catalysts FB and V5 with different heating rates.

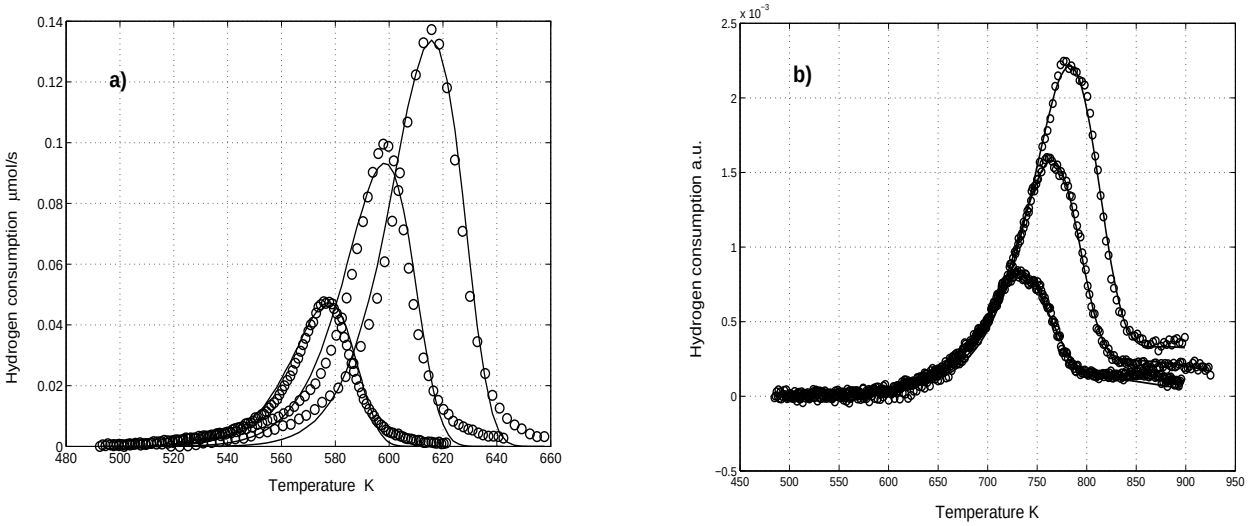

Figure 2.3. TPR data of the catalysts a) FB and b) V5 and the best-fit model solutions.

The kinetics of reduction of the catalysts was best described by the random nucleation (RN) model, the model of two-dimensional nuclei growth (2D N/NG) or a combination of these

(Tables 2.2 and 2.3). When the loading was sufficient, the reduction appeared to take place as a topochemical process on both supported oxide systems. For chromium catalysts the 2D N/NG mechanism was predominant for the samples ALD3, ALD4, ALD5 and FB. For vanadium catalysts the N/NG characteristics were exhibited in the reduction of the samples V5 and V11. The reduction of low-loaded samples (ALD1 and V2) was best described in terms of the homogeneous random nucleation model (RN). The TPR pattern reported by Koranne et al. [64] for a very low loaded vanadia on alumina catalyst (0.33 V/nm^2) showed two reduction peaks that seemed to merge for higher loaded samples (0.8–1.6 V/nm^2). This implies that differently reducing species may exist, despite the apparent single-process RN behaviour. Possibly, the reduction of the catalysts ALD2 and V5 formed an intermediate case between topochemical and homogeneous reduction. The 2D N/NG model provided a compromise fit for the TPR of the catalyst ALD2, and the main peak of V5 was best described by a combination of RN and 2D N/NG models.

Table 2.2. Best-fit kinetic models and Arrhenius parameters for the chromium oxide catalysts.

Sample	Model	E kJ/mol	A 1/s	k_2
ALD 1	RN	74.8 ± 0.6	$(5.0 \pm 0.6)*10^3$	
ALD2	2D N/NG	81.0 ± 1.0	$(6.6 \pm 1.3)*10^4$	
ALD3	2D N/NG	98.4 ± 0.8	$(3.5 \pm 0.6)*10^6$	
ALD4	2D N/NG	94.2 ± 0.8	$(2.4 \pm 0.4)*10^6$	
ALD5	2D N/NG	84.9 ± 0.9	$(4.1 \pm 0.7)*10^5$	
FB *)	2D N/NG	78 ± 2	$(1.8 \pm 0.7)*10^4$	$(3.6 \pm 1.5)*10^{-3}$

*) TPR of the catalyst FB was best described by the 3-parameter form of the N/NG model (II).

Table 2.3. Best-fit kinetic models and Arrhenius parameters for the vanadium oxide catalysts.

Sample	Process 1		Process 2		Process 3	
V2	**RN**					
	k_{ref} *) 1/s	E kJ/mol				
	$(6.8 \pm 0.2)*10^{-2}$	146 ± 3				
V5	**2D N/NG**		**RN**		**RN** (correction for the tailing)	
	k_{ref} 1/s	E kJ/mol	k_{ref} 1/s	E kJ/mol	k_{ref} 1/s	E kJ/mol
	$(7.2 \pm 0.1)*10^{-2}$	90 ± 2	$(9.5 \pm 0.3)*10^{-2}$	100 ± 2	$(10.5 \pm 0.2)*10^{-3}$	74 ± 3
V11	**2D N/NG**		**2D N/NG**			
	k_{ref} 1/s	E kJ/mol	k_{ref} 1/s	E kJ/mol		
	$(6.3 \pm 0.1)*10^{-2}$	87 ± 2	$(3.9 \pm 0.2)*10^{-3}$	119 ± 2		

*) The centred rate coefficient: $k(T) = k_{ref} \exp[E/R(1/T_{ref}-1/T)]$, where T_{ref} was 750 K.

Interpretation of the kinetic results

Molecular level factors that may allow the N/NG mechanism are now discussed. The model of two-dimensional nuclei growth implies that the reduction is initiated somewhere in the surface oxide layer, and the conversion proceeds to the surroundings as growing domains. Preconditions for the reduction mechanism assuming two-dimensional nuclei growth are that 1) supported oxide species interact with surrounding species and form a 'contiguous overlayer' and 2) the reactivity of the overlayer toward hydrogen is clearly higher at the boundary of the reduced and the non-reduced phase than at random locations inside non-reduced phase.

Both vanadium and chromium oxides are present as surface isolated or surface polymerised species with increasing degree of polymerisation as a function of loading, and they tend to form a two-dimensional overlayer on alumina [53,54]. A catalyst with close to monolayer content of active component can be envisaged as having an extensive polymeric network of oxide species on the support and the precondition (1) is thus satisfied. Low loaded catalysts (ALD1, V2) carry mainly isolated species, the precondition (1) is not fulfilled and the reduction takes place as a random process. For catalysts with intermediate chromium/vanadium content (ALD2, V5) the reduction likely takes place as an N/NG process in well-interconnected oxide domains, but any isolated species need to go through individual nucleation. Furthermore, the N/NG model fails to describe the situation where there is wide variability in the size of the reducible domains and the reaction is not allowed to advance freely owing to the abundant smaller domains. There is an obvious need for a kinetic model to properly account for this situation.

The greater propensity for reduction at the boundary of the reduced and non-reduced domains of the overlayer (precondition 2) could be adsorption-related. In the course of the reduction reaction, the reduced metal oxide sites might trap the gas phase hydrogen better than the oxidised sites and the reduction occurring next to the reduced sites would then be considerably favoured over the reduction at arbitrary locations in the old phase. Steric factors might also be involved: reduction leads to elimination of the short and rigid V=O bond present in dehydrated surface oxide species, which may improve the sticking probability of a hydrogen molecule to the neighbouring sites.

Initiation (nucleation) of the N/NG-based reduction could involve random nucleation events, which might be exceedingly rare at the temperature at which nuclei growth commences. Homogeneous nucleation could be so slow at these temperatures that the conversion caused by these events alone would not yet be measurable. Another possibility for initiation of the reduction is the existence of defective oxide species (such as non-redox Cr^{3+}, indicated in refs. [65, 66]) in the overlayer, which could trap hydrogen and act as starting points for the nuclei growth. This latter possibility excludes nucleation as a kinetic process and the overall reduction rate would be solely limited by the growth kinetics. The reduction of the catalysts ALD3- ALD5 appeared to be limited only by the nuclei growth, whereas the reduction of the catalyst FB may have been limited by both nucleation and nuclei growth (II).

The overlayer of chromia or vanadia is exposed to the heterogeneities of the alumina support. The active species may have different ways of binding to the support and the reducibility may vary among the species. The N/NG mechanism tends to even out the heterogeneity, since the reduction proceeds at the reaction boundary. The resulting kinetic parameters of the 2D N/NG model represent combined chemical kinetics of reduction.

Activation energies of reduction

The literature on reduction kinetics is briefly reviewed in the following and the reported activation energies and those obtained in this work are compared. Chromium [52,67,68,69,70] oxide catalysts have often been characterised on the basis of TPR experiments, and vanadium oxide catalysts have been investigated by both TPR [71, 72, 73, 74, 64, 75, 61, 49, 62, 63, 76] and isothermal reduction experiments [77, 78, 76]. However, reduction kinetics for these oxides, especially for chromium oxides, have seldom been investigated. It is known that both the support material [53, 75] and the loading [61, 62, 64, II, III] influence the reduction behaviour significantly, which further complicates comparisons. The support affects the reduction kinetics presumably through Cr–O–support and V–O–support bonds, while the loading affects the relative abundance of different species and their mode of organisation and thereby determines the predominant mechanism (topochemical or homogeneous). The activation energies of reduction for chromia and vanadia catalysts obtained in this work are compared not only with reported activation energies of reduction but with the activation energies of oxidative dehydrogenation (ODH)

of alkanes over the same catalysts. Comparison with ODH is meaningful because reduction is generally regarded as the rate-limiting step in ODH.

CrO_x/Al_2O_3

For the most part, the reduction kinetics in this work were best described with the 2D N/NG models with the activation energies of reduction between 80 and 100 kJ/mol (Table 2.2). The only kinetic study based on H_2-TPR data reported in the literature data concerns silica-supported chromia catalysts [52], so that the mechanisms and the activation energies cannot be compared. The reduction kinetics of chromia on alumina has been investigated under isothermal conditions with the use of carbon monoxide as the reducing agent and spectroscopic detection method (in-situ UV-vis- NIR spectroscopy) [79], and with the use of step-response method and mass spectrometric detection [80]. Both studies [79,80] postulated Langmuir–Hinshelwood-type multi-step kinetic models for the reduction reaction without topochemical characteristics. Bensalem et al. [79] report rate constants at different temperatures, but physically meaningful activation energy was not obtainable. Dekker et al. [80] report an activation energy of 95 kJ/mol for CO reduction of chromia on alumina (6.9 wt-% Cr). The value (98 kJ/mol) found in this work for the catalyst ALD3 (7.5 wt-% Cr) is close to their value.

The ODH of propane on chromia catalysts was recently investigated by Cherian et al. [81, 82] and the influence of the support, precursors and loading on the catalytic activity was reported. The activation energy of ODH of propane on CrO_x/Al_2O_3 catalysts, calculated from turnover frequencies (TOF) measured at several temperatures under differential conditions, was found to lie between 90 and 100 kJ/mol [82]. The energy appears to be of the same order of magnitude as the activation energies of reduction for the ALD series in this work. It would seem that the activation energy of reduction of CrO_x/Al_2O_3 is relatively insensitive to the reducing agent (H_2, CO, propane). Possibly then the activation energy reflects the breakage of the O–Cr bond in the rate-limiting step.

VO_x/Al_2O_3

The reduction kinetics of most of the vanadia catalysts of this work was described with combined models (Table 2.3). The activation energy for surface vanadia species reducing via the N/NG mechanism was roughly 90 kJ/mol. Model-fitting based kinetic analysis of the

reduction of vanadium oxide has been conducted in a few instances, and the results are collected in Table 2.4. As can be seen, there is variability in both the suggested mechanisms and the obtained activation energies. In addition to model fitting based kinetic analysis, TPR patterns of supported vanadia catalysts were deconvoluted by Gaussian curves [64, 74] and by a combination of random nucleation models [75]. The drawback of these kinds of deconvolutions is that they do not provide a proper basis for comparisons.

The only vanadia catalyst similar enough to those of this work to allow direct comparisons is that studied by Tarfaoui [49] (3.11 V/nm^2 vs. 3.7 V/nm^2 on V5). He [49] fitted various models based on gas–solid reaction mechanisms to the data of multiple TPR experiments. The smallest value of the object function was obtained for the model of two-dimensional nuclei growth with activation energy of 108 kJ/mol, but three other models were almost as good. The observations of the present work are thus in relatively good accord with his: two-dimensional nuclei growth seems to play a role, but it is not alone able to explain the reduction behaviour of the catalyst V5.

Table 2.4. Kinetic results for reduction of vanadium oxide catalysts.

Catalyst	Vanadium content V/nm^2	Reducing agent	Method of kinetic analysis	Activation Energy kJ/mol	Reference
VO_x/Al_2O_3	3.11	H_2	Model fitting to TPR data, 2D NG	108	Tarfaoui, [49]
VO_x/Al_2O_3 V-Mg-O	2.7 14.2	H_2	Model fitting to isothermal data, contracting sphere	145	Lopez Nieto et al. [76]
VO_x/TiO_2 V_2O_5	9.8	H_2	Model fitting to TPR data, 2D NG	59	Bosch and Sinot [83]
VO_x/TiO_2	~12	Propane	Model fitting to isothermal data, empirical model	82	Sloczynski [78]
VO_x/TiO_2	2	H_2	Kissinger, Random nucleation	98	Bulushev et al. [63]
V_2O_5	-	H_2	Kissinger, 3D N/NG	83	Ballivet –Tkatchenko and Delahay [73]

Activation energies for ODH reaction over alumina-supported vanadia have been reported, as calculated from reaction rates determined at different temperatures under differential conditions [84, 85], and as estimated in mechanistic kinetic modelling [86]. Argyle et al. [84] recently reported apparent activation energies of approximately 115 kJ/mol for ODH of both propane and ethane. The mechanistic kinetic analysis carried out by the same group [86] resulted in a similar value, 110±15 kJ/mol, for ODH of ethane. In earlier studies of LeBars et al. [85], apparent activation energy values for ODH of ethane were slightly above 100 kJ/mol. Mindful of the accuracy and limitations of this kind of determinations [84,85], and the

reported error bounds [86], we can conclude that the activation energies of reduction and the ODH reaction roughly coincide. The activation barrier of reduction is much the same irrespective of the reactant that reduces the vanadium cation in the process.

2.3 Conclusions

TPR provided a means for quantitative characterisation of the reduction behaviour of a series of supported chromium and vanadium oxide catalysts. Parameter estimation based on model fitting gave information about the underlying gas–solid reaction mechanisms and values of the kinetic parameters. Nucleation and nuclei growth played a role in the reduction of the chromia and vanadia catalysts where the oxide formed close to a monolayer on the support, whereas homogeneous random reduction of individual supported oxide species took place on low-loaded samples. Kinetics thus indirectly provides information on the mode of organisation of the oxide species.

In general, TPR technique might prove useful in understanding reactions taking place via redox mechanism. There seems to be an agreement between the activation energies of reduction of the chromia on alumina and vanadia on alumina catalysts and the activation energies of oxidative dehydrogenation on the same catalysts. Understanding of the reduction mechanism at microkinetic level might eventually lead to understanding of the decisive mechanistic step of ODH.

The frequently applied forms of the Avrami model are acknowledged to contain approximations. Some of the approximations can easily be abandoned, while some remain inherent in the construction of the theory.

Kinetic analysis of TPR data is valuable because the kinetic models 1) provide fundamental information on gas–solid interactions, 2) facilitate comparisons of TPR experiments carried out under different conditions by various research groups and 3) allow optimisation of pre-treatment procedures for oxide catalysts.

3 KINETIC ANALYSIS OF TPD

3.1 Temperature-programmed desorption and kinetic analysis

Temperature-programmed desorption (TPD, also known as flash desorption or thermal desorption spectroscopy, TDS) is one of the most useful temperature-programmed methods for characterisation of solid catalysts. The adsorption of the reactants precedes and the desorption of products follows the reaction on the catalytic surface in heterogeneous catalysis. Knowledge of the kinetics and energetics of these elementary reactions facilitates understanding of the catalytic cycle taking place on the catalyst.

In TPD studies a solid on which gas has been adsorbed is submitted to a programmed temperature rise and the amount of desorbing gas is continuously monitored. The temperature at which species are desorbed from the surface of a heated solid reflects the strength of the surface bonds. TPD (or flash desorption) was first described as a quantitative analytical tool for surface characterisation of low-surface-area samples in high vacuum by Redhead [26], who also showed the potential of the method to extract the adsorption energetics. TPD was proposed for the study of high-surface-area catalysts under carrier gas and ambient pressure by Amenomiya and Cvetanovic [25]. A vacuum set up is customarily used for surface science studies, whereas both flow and vacuum set-ups of TPD are used for catalysis studies. The dual nature of the TPD technique enables bridging of the material and pressure gaps in heterogeneous catalysis. Theory and applications of TPD have been reviewed by Cvetanovic and Amenomiya [29], Falconer and Schwarz [30,87], Lemaitre [32], Bhatia et al. [34], Tovbin [88] and Bennett [5].

TPD provides information that is relevant to catalytic properties. TPD data help in unravelling the complexity of gas–solid interactions. They characterise chemisorption or acidic properties with indication of the surface energetic heterogeneity and can be compared qualitatively with reference TPD patterns. The total amount desorbed can be related to the adsorption capacity, to the metal surface area and dispersion of the metal on supported metal catalysts and to the acid capacity of solid acid catalysts. TPD has also been suggested to be a good tool for determining site densities and reaction pathways on oxide catalysts [89]. Alongside the usual qualitative uses of TPD, quantitative kinetic and energetic information has been sought from TPD data.

Early methods to extract kinetic parameters included the variable heating rate method (analogous to the Kissinger method), the desorption rate isotherm method [90] (the second step of which is analogous to the Friedman method) and others [30]. De Jong and Niemantsverdriet [91] reviewed and tested approximate analysis procedures for TPD data. Rudzinski et al. [92] addressed the applicability of the Arrhenius plot methods to determine the surface energetic heterogeneity and pointed out their limitations. A very general way to extract kinetic parameters from TPD data is nonlinear regression analysis based on model fitting. Technical aspects of the nonlinear regression technique applied to analyse TPD data have been presented by Russell and Ekerdt [93]. The main challenge in the nonlinear regression method is not, however, the technical aspects but an adequate mathematical description of the physico-chemical system of TPD. The description covers both the intrinsic reaction rates and the mass transfer in the system.

In surface science studies the observed rate in TPD may directly reflect the intrinsic rate of unidirectional desorption and it is commonly described as the Polanyi–Wigner equation without readsorption [91]. Still, even in the most ideal desorption from single crystals, multipeak desorption patterns sometimes emerge as a manifestation of the intrinsic complexity of the system. Lateral interactions of the adsorbed species or different binding sites of the species may contribute to the multipeak TPD patterns. The extraction of kinetic parameters from TPD data obtained in UVH is reviewed by Niemantsverdriet [94].

Mathematical description of desorption kinetics for porous samples in flow set-ups is complicated by the superposition of several physico-chemical phenomena. Important methodological aspects of TPD from porous catalysts were dealt with during the 1980's [95,96,97,98,99]. Ibok and Ollis [95] developed a modified Weisz–Prater [100] criterion to assess the intraparticle diffusion limitations. Herz et al. [96] set up a more accurate mathematical description for kinetics of desorption from porous catalysts, which included rates of adsorption and desorption, rates of diffusion from the catalyst pellet and the CSTR reactor model. Both simulations and CO-TPD experiments on supported platinum indicated that adsorption equilibrium was closely approached in TPD and the significance of the readsorption was revealed. Rieck and Bell [97] established a simulation model with intrinsic adsorption and desorption kinetics, the catalyst particle balances with diffusion and a reactor model (CSTR or multiple CSTRs to account for packed bed behaviour). They studied the

influence of carrier gas flow rate and composition, the catalyst particle size, the length of the catalyst bed and spatially non-uniform adsorption for both first- and second-order desorption processes [97]. Their conclusions extended and confirmed the previous knowledge of TPD from porous catalysts. The physico-chemical models governing in TPD were nondimensionalised by Gorte [98] and Demmin and Gorte [99] and the effects of various experimental parameters were analysed. The analysis resulted in six dimensionless groups (ratios of characteristic rates of the system) for assessing the mass transfer phenomena in TPD [99]. Gorte's criterion for internal mass transfer limitation has been validated experimentally [101] and in simulation [97]. The intraparticle diffusion in TPD has also been evaluated by Huang et al. [102] in terms of the magnitude of the effectiveness factor, which takes into account temperature-dependent transport properties and readsorption.

Although models assuming intraparticle diffusion [103] and the integral reactor model [104,105] have occasionally been applied in the context of kinetic analysis of TPD, the CSTR model and the assumption of negligible intraparticle diffusion resistance are still customarily used in kinetic analysis of TPD data. The diffusional limitations and appropriate reactor model should be evaluated for each and every new TPD case.

In this work, adsorption/desorption of hydrogen on a supported nickel catalyst was investigated by H_2-TPD. The main objective was to set up methods and models applicable to investigation of the adsorption/desorption kinetics of this kind of system. As nickel is an active catalyst for hydrogenation, another objective was to provide information useful in microkinetic modelling of the hydrogenation of aromatics. An extensive review on nickel catalysts in the context of transient techniques has been provided by Falconer and Schwarz [87].

The TPD experiments were supplemented by static and pulse chemisorption experiments. A kinetic model to describe the adsorption and desorption during the TPD was developed and tested using nonlinear regression analysis. Adsorption equilibrium parameters and adsorption capacities were obtained through the kinetic analysis. The following section summarises the findings of publication (IV) and describes further tests of the assumptions made in the kinetic analysis.

3.2. Results and discussion

3.2.1 Experimental results

A commercial Ni/Al_2O_3 catalyst with 17 wt-% of Ni was investigated. Each TPD experiment consisted of the pre-treatment and five successive TPD runs, four of which were stable and reproducible. The heating rates in the successive TPD runs were 12, 6, 12, 18 and 12 K/min. The exposure of the catalyst to hydrogen in between the runs was conducted according to two procedures. The catalyst was cooled from the end temperature to the initial temperature in argon flow and this was followed by 10 min hydrogen flow over the catalyst at the initial temperature (procedure TPD I), or the catalyst was subjected to hydrogen flow already during the cooling (procedure TPD II). Experimental details of TPD and static and pulse chemisorption experiments can be found in (IV).

The TPD thermograms and total desorbed amounts of hydrogen were different for the procedures TPD I and TPD II. Figure 3.1, which depicts typical TPD patterns of the two procedures, clearly shows the differences in the qualitative characteristics of the thermograms. As a rule, more hydrogen desorbed when TPD II was applied. In experiments carried out with the TPD I procedure, the desorbed amount of hydrogen was less after adsorption at 303 K than at 323 K. Thus, for the TPD I series the amounts adsorbed did not follow the expected thermodynamic trend. Possibly this implies activated chemisorption. For the TPD II experiments, desorbed amounts of hydrogen increased with decreasing starting temperature.

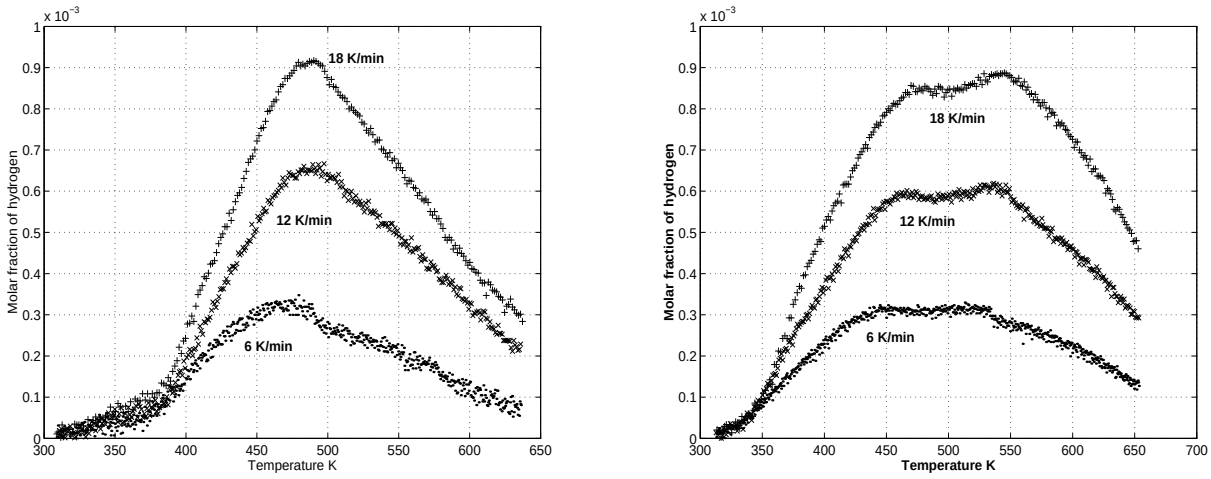

Figure 3.1. TPD patterns for the procedures a) TPD I and b) TPD II. The heating rates are indicated.

3.2.2. Kinetic models for TPD

The objective of the fourth study (IV) was to set up a kinetic model that would describe the observed desorption kinetics. To describe the qualitatively observed heterogeneity in the TPD patterns, n distinct types of adsorption sites were hypothesised. Re-adsorption was taken into account in the model.

The intraparticle diffusion limitation was carefully evaluated according to the criterion of Gorte [99] and found negligible. The reactor was modelled as a differential reactor. The dimensions of the catalyst bed in relation to the flow rate and the observed desorption dynamics constituted the grounds for the reactor selection. Simulations of similar kind of TPD experiment [104] indicated uniform surface coverage for the major part of the catalyst bed. If deviation from the uniform coverage at the entrance to the catalyst bed represents only a minor part of the bed then kinetic analysis based on uniform surface coverage is justified.

The main features of the model are summarised in the following. The differential reactor balance with hydrogen desorbing from n adsorption states becomes

$$Fx = -\sum_{i}^{n} \beta \; v_{m,i} \frac{d\theta_i}{dT} \tag{3.1}$$

where F stands for the total molar flow rate and x for the molar fraction of hydrogen, θ_i represents the surface coverage and v_{mi} the specific molar capacity of the i^{th} adsorption state. In TPD the sample temperature is raised at a constant rate:

$$\frac{dT}{dt} = \beta \tag{3.2}$$

Since x is the quantity observed in the TPD experiment and most conveniently compared with the model solution, the equation is further transformed by eliminating the system variables θ_i, i=1…n.

The adsorption/desorption related to each adsorption state i is assumed to be a second-order (dissociative) process with the distinct rate coefficients k_{ai} and k_{di}, respectively. If the re-adsorption in TPD is rapid enough to maintain the adsorption equilibrium, the surface coverage of the i^{th} adsorption state can be expressed as a function of the gas phase composition:

$$\theta_i = \frac{(K_i x)^{1/2}}{1+(K_i x)^{1/2}} \tag{3.3}$$

where K_i is the adsorption equilibrium constant for the ith adsorption state. All the adsorption states are in simultaneous equilibrium with the gas phase hydrogen, molar fraction x. The temperature dependence of K_i is expressed in line with the kinetic theory of gases:

$$K_i = \frac{A_i}{\sqrt{T}} \exp\left(\frac{-\Delta H_i}{RT}\right) \tag{3.4}$$

where A_i is the pre-exponential constant, ΔH_i is the adsorption enthalpy and R is the gas constant.

Equation (3.1) can now be expressed in the following form:

$$Fx = -\sum_{i=1}^{n} \nu_{m,i} \beta \left(\frac{\partial \theta_i}{\partial K_i}\frac{dK_i}{dT} + \frac{\partial \theta_i}{\partial x}\frac{dx}{dT}\right) = -\sum_{i=1}^{n} \nu_{m,i} \beta \frac{\partial \theta_i}{\partial K_i}\frac{dK_i}{dT} - \frac{dx}{dT}\left(\sum_{i=1}^{n} \nu_{m,i} \beta \frac{\partial \theta_i}{\partial x}\right) \tag{3.5}$$

This becomes an ordinary first-order differential equation for x:

$$\frac{dx}{dT} = \frac{Fx/\beta + \sum_{i=1}^{n} \nu_{m,i} \frac{\partial \theta_i}{\partial K_i}\frac{dK_i}{dT}}{-\sum_{i=1}^{n} \nu_{m,i} \frac{\partial \theta_i}{\partial x}} \tag{3.6}$$

The surface coverage variables θ_i are eliminated from (3.6) by assigning the derivatives

$$\frac{\partial \theta_i}{\partial K_i} = \frac{1/2\, K_i^{-1/2} x^{1/2}}{\left(1+(K_i x)^{1/2}\right)^2} \tag{3.7}$$

$$\frac{dK_i}{dT} = A_i T^{-3/2} \exp\left(\frac{-\Delta H_i}{RT}\right)\left(-1/2 + \frac{\Delta H_i}{RT}\right) \tag{3.8}$$

$$\frac{\partial \theta_i}{\partial x} = \frac{1/2\, K_i^{1/2} x^{-1/2}}{\left(1+(K_i x)^{1/2}\right)^2} \tag{3.9}$$

The numerical solution of model (3.6.) can be readily tested against experimental TPD data by model fitting, which results in estimates for A_i, ΔH_i and ν_{mi} for each adsorption state i. The initial value essential for the solution of (3.6.) is carefully assigned to match the experimental initial molar fraction.

Multipeak characteristics in TPD patterns are sometimes attributed to lateral interactions between the adsorbed species, which are customarily accounted for by allowing the

adsorption energy and entropy to vary with coverage. The approach taken in this work ignores possible lateral interactions.

The parameter estimation in this work, including numerical solution of (3.6.), was implemented in MATLAB® 6. Multiple TPD curves with various starting temperatures and heating rates (related to both TPD I and II procedures) were used for the parameter estimation. The quasi-equilibrium adsorption model with two adsorption states provided an adequate fit for the data collected according to the procedures TPD I and TPD II. Parameters were well-identified and of physically reasonable order of magnitude. Tables 3.1 and 3.2 report the estimated adsorption parameters and Figure 3.2 displays the best-fit model solution and the experimental data. For both TPD procedures (Tables 3.1 and 3.2) the adsorption state 2 can be related to one specific adsorption state, but state 1 appears to be different for the two TPD procedures. This conclusion is explained in (IV).

Table 3. 1. Results of kinetic modelling with a two-state model for TPD I experiments with T_0=323 and 343 K and β = 6, 12, and17 K/min.

State index (i)	Parameter estimates		
	$A_{i,ref}$ ($K^{1/2}$)	ΔH_i (kJ/mol)	v_{mi} (mmol/ g_{Ni})
1	(2.3 ± 0.2)e4	-122 ± 3	0.51 ± 0.03
2	(3.6 ± 0.3)e5	-63 ± 1	1.07 ± 0.03

$K_i = A_{i,ref} * T^{-1/2} * \exp(\Delta H_i / R(1/T_{ref} - 1/T))$, where T_{ref}= 475 K

Table 3.2. Results of kinetic modelling with a two-state model for TPD II experiments with T_0=323 and 343 K and β = 6, 12, and17 K/min.

State index (i)	Parameter estimates		
	$A_{i,ref}$ ($K^{1/2}$)	ΔH_i (kJ/mol)	v_{mi} (mmol/ g_{Ni})
1	(2.2 ± 0.4)e3	-117 ± 4	0.29 ± 0.01
2	(5.9 ± 0.4)e5	-72 ± 1	1.41 ± 0.02

Validation and testing

To further evaluate the kinetic analysis of the TPD data for the H_2- Ni/Al_2O_3 system (IV), the two most significant assumptions made in the analysis, namely the differential reactor assumption and the quasi-equilibrium adsorption assumption, were relaxed to see their influence on the results.

Integral reactor model and quasi-equilibrium adsorption

TPD was simulated with the previously estimated adsorption parameters and quasi-equilibrium adsorption but using an integral reactor model in order to see how the solution differed from that given by the differential reactor model. (The integral reactor model was implemented by connecting multiple differential reactor models in series and utilising the quasi-equilibrium assumption, eqs. 3.3, 3.7-3.9) A uniform molar fraction corresponding to the experimental value was assigned as the initial value for the solution. The difference between the simulated results obtained with the different reactor models was minor for some conditions but significant for others. The parameter estimation for the TPD data was consequently carried out with use of a complete integral reactor model. The agreement between these and earlier parameter estimates was good though not outstanding. While the simulations showed some deviations from uniform concentration, the order of magnitude and the interpretation of the results from original parameter estimation remained essentially the same.

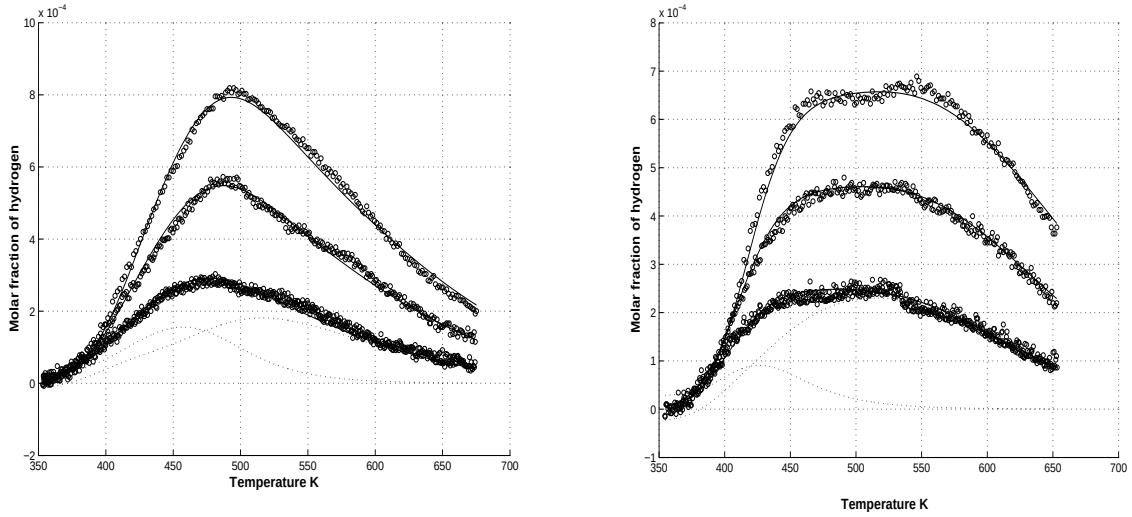

Fig. 3.2. Experimental data and best-fit model solutions for a) TPD I and b) TPD II. (T_0=343, β=6, 12, 18 K/min)

Integral reactor model and independent adsorption and desorption reactions

The simulation was next carried out with adsorption and desorption processes but without the quasi-equilibrium assumption. Independent adsorption and desorption kinetics were applied with the integral reactor model in the parameter estimation to see whether this description of the model was closer to the experimental results than with the quasi-equilibrium assumption. An evolutionary approach was necessary since the new model

contained ten degrees of freedom instead of the previous six. The convergence of the problem was poor and it was necessary to fully utilise the information obtained from the quasi-equilibrium model. First, the independent kinetics was applied with the gradientless reactor model to estimate reasonable initial guesses for the parameters. The ratios of pre-exponentials of adsorption and desorption and the adsorption capacities were fixed on the basis of the previously estimated adsorption equilibrium parameters, the activation energies of desorption values were assigned the previous -ΔH estimates, and adsorption was treated as non-activated at this stage. The initial value for the gas-phase composition was assigned to match the measured one and the surface coverage values were calculated from the previously modelled quasi-equilibrium. Finally, all ten parameters were adjusted freely in the model fitting. These parameter estimates were then assigned as initial guesses for the parameter estimation incorporating the integral reactor model. The new model did not provide a better description: the fit was essentially as good as with the quasi-equilibrium model. The estimated parameters were not unique: the adsorption and desorption cannot be identified as independent processes for this system.

Model (3.6) appears to be suitable for describing the interaction between a gas and a macroporous supported metal catalyst during TPD provided that the re-adsorption is fast, and axial and intraparticle gradients are negligible. The application of the model may also be useful as an intermediate step in model development incorporating a more general reactor model.

Consistency of the TPD results

The experimental data and the results of kinetic analysis (IV) provided wide information on the adsorption behaviour of hydrogen on the nickel catalyst. The amounts desorbed in the TPD I experiments agreed with the irreversible adsorption capacity, and those desorbed in TPD II with the total adsorption capacity determined using the static chemisorption. The sum of the estimated capacities of the adsorption states was also meaningful in the light of these values. The TPD results suggested the existence of two adsorption states. Likewise, previous investigations on the nickel/hydrogen adsorption system carried out by different methods have indicated at least two adsorption states [106]. The adsorption enthalpies estimated on the basis of kinetic analysis of the TPD experiments (ΔH= -63, -122 kJ/mol) are

in broad agreement with the adsorption enthalpy values for hydrogen on nickel reported in the literature (Table 3.3) and are of reasonable order of magnitude.

Table 3.3. Adsorption enthalpies of hydrogen on nickel surfaces.

Surface	$-\Delta H_a$ kJ/mol	Method	Reference
Ni(100)	96	TPD, UVH	Christman et al. [107]
Ni(110)	90	"	"
Ni(111)	96	"	"
24.3% Ni/SiO_2	35.9, 48.0, 60.8, 85.4, 123.4, 170	TPD	Konvalinka et al [108]
~50% Ni/SiO_2	55–89	TPD	Lee et al. [109]
Ni/SiO_2	82–84	TPD	Weathterbee, Bartholomew [110]
14% Ni/Al_2O_3	70, 125	TPD	"
17% Ni/Al_2O_3	124.3, 222.5, 413	TPD, UVH	Smeds et al [111]
Polycrystalline Ni	60–125	Calorimetric analysis	Wedler [112]
Ni/SiO_2	50–110	Calorimetric analysis	Prinsloo, Gravelle [113]
Ni/kieselguhr	57.7	Pulse chromatographic analysis	Padberg, Smith [114]
Ni catalyst	58.5	"	Damiani et al. [115]

3.2.3. Pulse chemisorption

The pulse chemisorption experiments provided complementary information on the adsorption and desorption kinetics. Fifteen hydrogen pulses were introduced into the argon carrier gas at three different temperatures and the response pulses after the reactor were measured. The catalyst adsorbed the first few pulses completely and subsequent response pulses increased one by one finally obtaining constant concentration behaviour as a function of time. Qualitative interpretations of the pulse chemisorption data showed that all adsorption was rapid, and reversible adsorption occurred at each temperature studied. In particular, the reversible adsorption observed at 305 K was related to weaker adsorption than was encountered in the TPD experiments. Preliminary parameter estimation by model fitting was also conducted for the pulse chemisorption data, but proper identifiability requires more experiments. The pulse chemisorption results independently supported the assumption of rapid readsorption to the medium and strong chemisorption states from the

temperature 338 K on, which further validates the quasi-equilibrium treatment of the TPD data.

3.3. Conclusions

Wide experimental data on the adsorption properties of a commercial Ni/Al_2O_3 catalyst were collected by H_2-TPD, static chemisorption and pulse chemisorption. Kinetic analysis of the TPD data was carried out by nonlinear regression analysis. TPD data were analysed in terms of a kinetic model assuming quasi-equilibrium adsorption to multiple adsorption states. Multiple-state quasi-equilibrium adsorption combined with the differential reactor model resulted in a first-order nonlinear differential equation, the numerical solution of which can be directly applied in model-fitting based nonlinear regression analysis.

The temperature at which the catalyst was exposed to hydrogen had an influence on the amounts adsorbed and on the nature of TPD patterns. Two adsorption states were sufficient to describe the surface heterogeneity in the temperature range 323-673 K. The estimated enthalpies for adsorption ranged from -63 to -122 kJ/mol. The adsorption capacities of TPD agreed with the ones determined by static chemisorption.

This case study demonstrates that adsorption energetics for porous catalyst samples can be consistently extracted from TPD experiments. With the existing computing resources the possible superposition of different physico-chemical phenomena should not constitute a problem, so long as relevant phenomena are properly accounted for in the model. This kind of kinetic analysis of TPD could precede a microkinetic modelling of a heterogeneously catalysed reaction. The results of this study are potentially useful in the study of hydrogenation kinetics on this particular catalyst.

4 KINETIC ANALYSIS OF TPO

4.1 Kinetic analysis of coke combustion

Coke refers to undefined hydrogen-deficient organic compounds that deposit on catalysts during hydrocarbon conversions. The coke causes catalyst deactivation by occupying the active sites and blocking the catalyst pores. The process of deactivation is especially rapid in fluid catalytic cracking (FCC), making catalyst regeneration an essential part of the operation of FCC units [116]. In FCC, regeneration restores the catalyst activity and provides the heat required for feed evaporation and for compensating for the endothermic cracking reactions. In the regeneration coke oxidises to form carbon dioxide, along with carbon monoxide and water.

The design and optimisation of a regeneration unit requires an extensive simulation model, which includes a kinetic model of regeneration providing predictions of the intrinsic rates of oxidation reactions as a function of the process conditions. The simulation model provides a means to reduce operational and investment costs of the process and to optimise the operation so that it is safe and environmentally acceptable. The conditions of interest for the regenerator of an FCC unit cover oxygen concentrations of 1–21% and temperatures of 500–800 ºC. These are the conditions in which the kinetic model should adequately describe the rates of oxidation reactions.

Publication V deals with the regeneration kinetics of the commercial FCC catalyst being used in the pilot unit for the new FCC technology NExCC™[117]. The nature of coke is affected by the cracking conditions [118], type of catalyst, feed composition and ageing [119], which necessitates process-specific kinetic models of regeneration. The feed type of the cracking unit (light gas oil with boiling point 300-400 °C) and the cracking conditions (higher temperature, shorter contact time than in conventional FCC) resulted in low coke content (0.18 wt-%). The oxidation of the coke was performed in a fixed bed reactor in temperature-programmed mode (TPO). The evolved CO_2 and CO were detected separately with a procedure, first suggested by Fung and Querini [120]. The detection was based on separating CO_2 from total carbon oxides ($CO+CO_2$) by absorbing CO_2 into an ascarite filter, converting the resulting CO and the by-passed $CO+CO_2$ streams to methane and by

analysing the two streams using flame ionisation detector (FID). The validity of the detection method naturally requires that 1) no other volatile carbon species are present, 2) the retention of CO_2 on the filter is quantitative and 3) the methanator kinetics is more rapid than the coke oxidation kinetics. For experimental details the reader is referred to (V).

Various thermoanalytical techniques have been utilised to characterise coke [121]. The application of temperature-programmed oxidation (TPO) experiments for the determination of the kinetics has been described by Querini and Fung [121, 122]. TPO continues to be an important tool for qualitative characterisation of coke [123]. Kinetic analysis of TPO data requires consideration of the aspects discussed in section 1.4. In the ideal case, the intrinsic coke combustion kinetics is directly reflected in the experimental results of oxidation and can be extracted as such. The coke burn-off kinetics may, however, be limited by the diffusion of oxygen into the catalyst pores [124]. The effective diffusivity of gases in the catalyst customarily decreases with coke deposition [125].

The rate of coke oxidation is also be affected by topochemical characteristics. The reaction can take place as a shell-progressive process in the catalyst pellet [124] or on the exposed surface of larger three-dimensional or layered coke structures [122]. In these cases the intrinsic kinetics needs to be combined with the dynamics of the reactive surface. In some cases, different pore models can be combined with intrinsic kinetics and used in the kinetic analysis of catalyst regeneration [126]. If there is wide variability in the shapes, sizes and porosities of the deposited coke particles (heterogeneous coke morphology), complex TPO patterns arise and resolution of the intrinsic kinetics and the topochemical features may not be possible. A non-ideal TPO pattern due to the heterogeneous morphology (changing order with respect to coke) was demonstrated in a simulation of Querini and Fung [122].

In most studies on regeneration kinetics the intrinsic kinetics is still directly assessed under the assumption that topochemical and diffusional restrictions are negligible. The global kinetics is commonly described by applying homogeneous power-law rate expressions, in which the reaction orders with respect to the coke content, and the partial pressure (or concentration) of oxygen, are either equal to one or they are adjusted between zero and one [122,127,128,129,130]. Complex TPO spectra have commonly been interpreted as representing the oxidation of several types of coke with different reactivities, and the

thermograms have been deconvoluted by a linear combination of power-law expressions [122]. This approach can result in a good prediction for the coke combustion kinetics if adjustable parameters are determined from an informative set of experimental data [122]. However, a physico-chemical interpretation is not easily assigned to the combined power-law models with fractional reaction orders for coke or oxygen.

Even chemically homogeneous coke can generate complex TPO patterns if multiple reaction steps are contributing to overall rate. Homogeneous semi-mechanistic approaches with multistep reaction pathways have been introduced to interpret the complex TPO spectra of coked cracking catalysts [131,132,133,134] and charcoal and graphite [135]. Brown and co-workers [131,132,133,134,135] introduced a five-step kinetic scheme with a metastable dioxygen surface complex and a dissociated stable surface oxygen species as intermediates between the coke and the gaseous carbon oxides. There were two pathways for both CO and CO_2 evolution. The proposed mechanism provided a good simulation for the formation of CO and CO_2 during TPO. Both CO evolution rates were independent of the partial pressure of oxygen, while CO_2 evolution rates indicated 0.75-order O_2-dependence [133].

4.2 Results and discussion

The thermograms for our experiments, the evolutions of CO and CO_2 as a function of temperature, are shown in Figure 4.1. Smooth single-peak thermograms were obtained in every measurement. The formations of CO and CO_2 appeared to be highly correlated, with almost concurrent rate maxima. The apparent activation energies (E) were extracted from the experimental data by the Kissinger method [39]. This was done separately for the three oxygen concentrations and resulted values of activation energies of about 145 kJ/mol for the formation of CO and between 120 and 180 kJ/mol for the formation of CO_2. The prerequisites for a correct Kissinger analysis possibly are not fulfilled for this system.

Kinetic analysis of the results (V) was established on the following assumptions: 1) the TPO experiments took place in a kinetically controlled regime, 2) the sample temperature was well-controlled, and 3) the coke constituted a carbon reserve of uniform nature (one 'type of coke'). Assumptions 1 and 2 were supported by observations and additional calculations (V)

and assumption 3 was supported by the fact that the coke content of the samples was exceedingly low and the measured TPO patterns showed ideal characteristics.

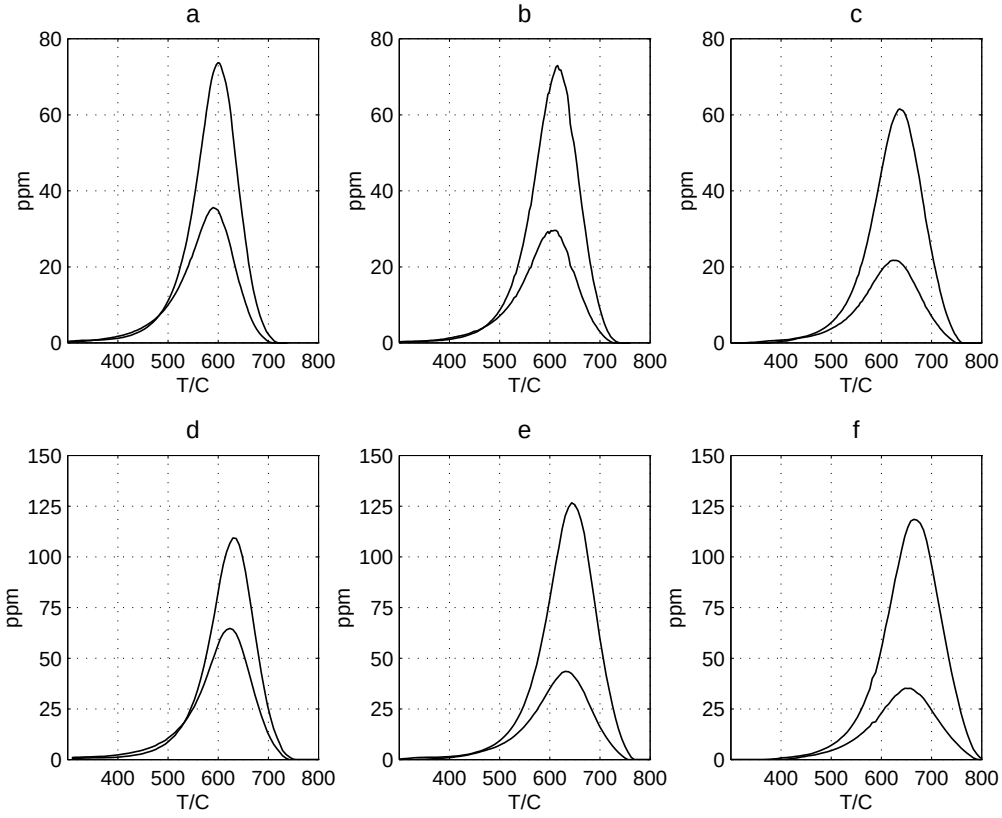

Figure 4.1. TPO thermograms: concentrations (in ppm) as a function of temperature a) 2.0% O_2, 5 K/min, b) 1.0 % O_2, 5 K/min, c) 0.5% O_2, 5 K/min, d) 2.0% O_2, 10 K/min, e) 1.0% O_2, 10 K/min, f) 0.5% O_2, 10 K/min. Upper curves in each figure represent CO and lower ones CO_2.

The dynamic CSTR reactor model was introduced for the nonlinear-regression-based kinetic analysis. The consumption of oxygen was minimal (instantaneous maximum conversion < 2 % in all experiments) and thus the reactor operated gradientlessly. Different kinetic expressions were embedded in the reactor model and parameter estimation was carried out in MATLAB® environment.

The kinetic analysis concentrated on homogeneous semi-mechanistic reaction models, three of which are collected in Table 4.1 (V). *S* denotes the molar amount of coke, S^* the molar amount of stable surface oxide, $[O_2]$ the bulk concentration of oxygen, *A* the pre-exponential factor, *E* the activation energy, *K(T)* the equilibrium constant of oxygen adsorption, and *n* the reaction order with respect to oxygen. Each of the reaction steps in schemes I-III might be composed of several elementary steps.

Table 4.1. Kinetic models for coke oxidation.

Model I
$coke + O_2 \rightarrow CO \qquad r_{CO} = A_1 \exp\left(\frac{-E_1}{RT}\right) S [O_2]^{n1}$
$coke + O_2 \rightarrow CO_2 \qquad r_{CO_2} = A_2 \exp\left(\frac{-E_2}{RT}\right) S [O_2]^{n2}$
Model II
$coke + O_2 \rightarrow surface\ oxide \qquad r_0 = A_0 \exp\left(\frac{-E_0}{RT}\right) S [O_2]^{n0}$
$surface\ oxide\ (+ O_2) \rightarrow CO \qquad r_1 = A_1 \exp\left(\frac{-E_1}{RT}\right) S^* [O_2]^{n1}$
$surface\ oxide\ (+ O_2) \rightarrow CO_2 \qquad r_2 = A_2 \exp\left(\frac{-E_2}{RT}\right) S^* [O_2]^{n2}$
Model III
$coke + O_2 \leftrightarrow surface\ oxide$
$surface\ oxide \rightarrow CO \qquad r_1 = A_1 \exp\left(\frac{-E_1}{RT}\right) \frac{(K(T)[O_2])^{1/2}}{1+(K(T)[O_2])^{1/2}} S$
$surface\ oxide\ (+O_2) \rightarrow CO_2 \qquad r_2 = A_2 \exp\left(\frac{-E_2}{RT}\right) \frac{(K(T)[O_2])^{1/2}}{1+(K(T)[O_2])^{1/2}} S [O_2]^n$

Model I represents the simplest power-law kinetics. The two reactions share a common reserve of coke, but they are otherwise independent. The Arrhenius parameters and the reaction orders with respect to oxygen were estimated, and the reaction order with respect to the coke was assigned as one. Model I gave a good description of the experimental data (Figure 4.2, **r**oot **m**ean **s**quare **e**rror, rmse ~ 1.60 ppm) and the parameters were well-identified. Table 4.2 reports the parameter estimates with their 95% confidence intervals. The reaction order with respect to oxygen was close to 0.6 for both reactions, but, as expected, was slightly higher for the formation of CO_2. The activation energy of the CO formation was close to the result of the Kissinger analysis (146 kJ/mol). Additional tests were carried out by using first-order dependence for both oxygen and coke in Model I. This model did not perform as well as the model with fractional orders for oxygen (rmse ~ 3.27 ppm). Additional calculations also indicated that the first-order dependence on coke was optimal. The direct proportionality of the rate of reaction to the remaining amount of coke supports the assumption that the coke was well dispersed on the samples.

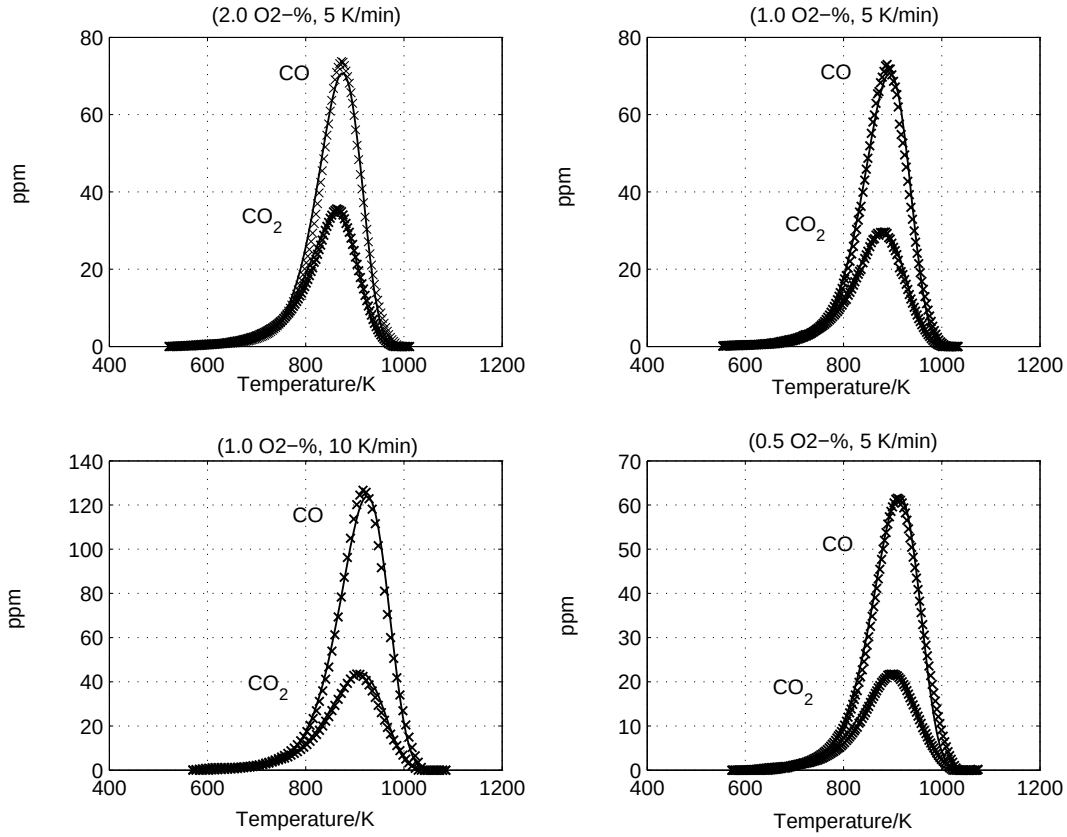

Figure 4.2. Best-fit solution of Model I (continuous line) and experimental TPO data.

Table 4.2. Parameter estimates for Model I.

A_1 [μmol/dm^3]$^{-n1}$ min^{-1}	(1.1 ± 0.1) *10^6
E_1 kJ/mol	146.2± 0.8
n_1	0.58 ± 0.02
A_2 [μmol/dm^3]$^{-n2}$min^{-1}	(3.4 ± 0.6) *10^3
E_2 kJ/mol	112 ± 1
n_2	0.64± 0.02

Model II (Table 4.1) introduced an additional reaction step. Since the reactions of CO and CO_2 formation were apparently highly correlated in the experimental data and the reaction orders of O_2 were closely similar for CO and CO_2 formation in Model I, the reaction was described to proceed via an intermediate surface oxide that could transform to either gaseous CO or gaseous CO_2. This model performed equally as well as Model I (rmse ~ 1.59 ppm). However some parameters, especially the Arrhenius parameters for CO_2 formation, were not properly identified. The full parametric model contained too many degrees of freedom and thus loose, unnecessary dynamics. The reaction orders with respect to oxygen (n_1 and n_2 ~0, (V)) suggested that the rate-determining steps of CO and CO_2 evolution from the intermediate oxide were practically independent of oxygen concentration, whereas the

formation rate of surface oxide was of order 0.6 with respect to oxygen in accordance with Model I. Model II was thus simplified by omitting n_1 and n_2 from the parameter estimation and by presenting the rate coefficient for formation of CO_2 as a constant, k_2. The revision of Model II did not cause deterioration in the fit (rmse ~ 1.59 ppm). The estimated parameters for the revised Model II are reported in Table 4.3. Model II represents a reaction with a rate-determining surface oxide formation step and subsequent low-activated formation of gaseous products. The rate determining steps related to the release of CO and CO_2 from the surface intermediate do not require more oxygen.

Table 4.3. Parameter estimates for Model II.

A_0 [μmol/dm^3]$^{-n0}$min^{-1}	(3.0 ± 0.3) * 10^5
E_0 kJ/mol	134.9± 0.8
n_0	0.60 ± 0.1
A_1 1/min	2.0 * 10^2 ± l.c
E_1 kJ/mol	37 ± 2
K_2 1/min	28 ± l.c

Table 4.4. Parameter estimates for Model III.

A_1 dm^3/(μmol min)	3.1 *10^{10} ± l.c.
E_1 kJ/mol	145.1 ± 0.8
A_2 dm^3/(μmol min)	9.5 *10^7 ± l.c.
E_2 kJ/mol	109 ± 1
K_3 dm^3/μmol	2.3 *10^{-9} ± l.c.

l.c. = large confidence interval

Model III was formulated in an attempt to explain the reaction order of 0.6 obtained for oxygen. Model III assumed that 'an intermediate surface oxide' formed in a fast equilibrium reaction and then further transformed to gas-phase CO and CO_2. The surface oxide formation was described with the Langmuir model for dissociative adsorption of oxygen on the carbon sites. The degrees of freedom of Model III were reduced to minimum by omitting the temperature dependence of the equilibrium constant. The reaction order with respect to oxygen became insignificant for the evolution of gaseous CO_2 from the surface intermediate and it was also left out of the parameter estimation. Surprisingly, the reduced five-parameter model was still able to describe the experimental TPO data (rmse ~ 1.79 ppm). The parameters are reported in Table 4.4. The activation energy values were almost the same as those for Model I.

Comparison of the obtained kinetic results with literature values is not straightforward because of the case-specific nature of coke. Moreover, most reports do not distinguish between the formations of CO and CO_2 but treat them together. Published apparent activation energy values for the overall coke combustion over a cracking catalyst or similar catalysts, without distinction of CO and CO_2, are reported in Table 4.5. The orders of magnitude of the activation energies (Table 4.5) and of those obtained in this work are the same.

Table 4.5. Activation energies for coke combustion on silica-alumina catalysts.

E kJ/mol	Catalyst	Reference
130-143	Silica-alumina catalyst for isomeration	127
156-158	Laboratory coked FCC catalyst	136
119	Commercial FCC equilibrium catalyst	136
157	Different oxides e.g. silica-alumina	137
161	FCC catalyst	138
125	FCC catalyst	129

Li and co-workers [133, 134] have reported results of kinetic modelling of TPO data for cracking catalysts. Their five-step reaction scheme included steps corresponding to the reactions of Model I, so that our activation energies can be compared with theirs. Their activation energy values for the regeneration of a spent FCC catalyst were 131 ± 5 and 98 ± 5 kJ/mol for the formation of CO and CO_2, respectively [133]. The values are fairly close to the values of Models I and III. Li et al. [134] also investigated laboratory-coked catalysts with TPO. The catalysts were deactivated by cracking 1-octene at different temperatures (200–600 ºC). They found that the cracking temperature clearly affected the coke formation and consequently the kinetic parameters obtained by analysing the TPO data. The kinetic analysis of the TPO data of the catalyst deactivated at 600 ºC resulted in activation energy values of 138 ± 3 and 101 ± 4 kJ/mol for the formation of CO and CO_2, respectively [134]. Both values are just barely below those obtained with Models I and III. It is noteworthy that 1) the reaction scheme in refs. 133 and 134 also includes other reactions, 2) the oxygen dependence of the reaction rate is expressed as partial pressure, which is not fully equivalent to the molar concentration unit used in this work and 3) the reaction orders with respect to oxygen appear to be different.

The kinetic analysis of this work (V) can be summarised as follows: The experimental TPO data could be regressed by three homogeneous kinetic models. Even two independent power-law-type kinetic models adequately described the rate of formation of CO and CO_2. This suggests that the coke is indeed of uniform nature and it is likely that the rates of formation of CO and CO_2 are mainly controlled by a single rate-determining step each. A common intermediate surface oxide species might explain the observed concurrence of the evolution of CO and CO_2, even though the introduction of a third independent reaction describing the formation of the intermediate did not substantially improve the fit and tended to add unnecessary dynamics. A fractional reaction order (0.6) for oxygen was obtained with Models I and II. An explanation for the fractional order of oxygen could be dissociative

coordination of oxygen on the carbon sites to form an intermediate that is subsequently involved in the rate-determining steps for the evolution of gaseous CO and CO_2 (Model III). The present observations on the coke combustion reaction did not encourage the introduction of further mechanistic complexity.

The TPO method appears to be a useful tool for kinetic determinations of oxidation reactions. Two observations may be made on the application of TPO for engineering purposes: 1) A wider set of oxygen concentrations in experiments is desirable for predictions that will be reliable under the whole range of practical conditions, and 2) thermograms of water should also be measured and analysed in terms of a kinetic model, since the oxidation of hydrogen is of importance in the heat balance. Application of TPO for fundamental understanding of oxidation reactions is challenging since coke is not one specific substance but comprises different compounds and in some cases different morphologies. Chemical and physical characterisation of the catalyst and the coke could provide additional insight. Elucidation of intrinsic mechanistic details would greatly benefit from measurement of the thermograms of oxygen and water during TPO to establish the complete oxygen balance.

4.3 Conclusions

Kinetic analysis of coke combustion in low oxygen concentrations was conducted with the aid of TPO experiments. The formation of both CO and CO_2 was found to likely involve a single rate-determining step. Power-law models with first-order for coke and approximately 0.6-order for oxygen accurately described the rates of CO and CO_2 evolution. The obtained activation energies were 146 and 112 kJ/mol, respectively. The fractional reaction order for oxygen could result from dissociative adsorption of oxygen on the carbon sites. The estimated values of kinetic parameters are process-specific and closely related to the type of feed, the catalyst type and the cracking conditions.

TPO experiments provide overall evolution rates of gaseous products and enable a description of the main dynamics of coke combustion as a function of process conditions. This case study suggests that TPO is a useful tool to extract the kinetics of catalyst regeneration for engineering purposes.

5 ASSESSMENT OF KINETIC ANALYSIS OF TEMPERATURE-PROGRAMMED REACTIONS

There is a common methodological basis for kinetic analysis applied to temperature-programmed reactions, even though the intrinsic phenomena differ. In this chapter, characteristics of the kinetic analysis of temperature-programmed reactions are discussed on the basis of the findings of the case studies I-V. The special characteristics of kinetic analysis originating of the properties of gas–solid reactions and the methods to extract kinetic information about these reactions are reported and discussed with reference to the relevant literature.

5.1. Level of information obtainable from TPD, TPR and TPO

The bulk concentrations, which reflect the intrinsic kinetics of gas–solid interactions, are equivalently measured for the three temperature-programmed techniques. Even though the temperature-programmed techniques are equivalent in many respects, kinetic analyses of TPD, TPR and TPO data have the potential to provide information at different levels of detail. The complexity of gas–solid interactions in the systems increases in the order TPD, TPR and TPO, as measured by the nature of the reactive solid, the number of gaseous components and the number of reactions involved. The complexity reduces the chances of tracing back the underlying intrinsic phenomena and correctly assigning them. The utility of TPx methods can be enhanced by monitoring as many as possible of the species involved in the reactions. Interpretation of TPx data is also greatly assisted by the availability of complementary catalyst characterisation information.

TPD allows assessment of intrinsic gas–solid interaction: either desorption or both adsorption and desorption. This information is directly usable in the microkinetic modelling of heterogeneously catalysed reactions. Alternatively the kinetic analysis provides a detailed adsorptive fingerprint of the material independent of process conditions.

Analysis of the TPR of oxides provides at least the global reduction kinetics. If the topochemistry is adequately described, TPR gives information on the intrinsic rate-determining step(s) of a gas–solid reaction. The rate-determining step may even be identified

by comparing the activation energy of reduction with the bond energies of candidate bonds to be broken in the reduction.

TPO allows assessment of global coke oxidation kinetics, valuable for engineering designs. The kinetic parameters cannot be related to elementary reactions of microkinetic significance unless the identity of the coke compounds is revealed.

5.2 Challenges in kinetic analysis of TPx data

Thermoanalytical data is often complex due to the heterogeneity and non-uniformity of real materials. At best, the simplified kinetic models presently available capture the major system dynamics. Simplifying assumptions do not necessarily worsen the ability of a model to describe experimental results, so long as the material heterogeneities do not manifest themselves in the experimental data or the averaged situation represents well the overall dynamics. A well-known example of this is the application of the Langmuir–Hinshelwood models to describe the chemical kinetics of heterogeneous catalytic reactions: even though the catalytic material is characterised by structural heterogeneities, the actual surface reaction may still take place on a relatively limited and uniform group of surface sites [139]. Furthermore, in a heterogeneously catalysed reaction, the surface coverages of the reactants may not change dramatically even though the macroscopic process parameters are varied. A TPx experiment differs essentially from this: in the course of the reaction the conversion of solid increases from zero to complete (TPR/TPO etc) or the surface coverage evolves from complete to zero (TPD). The kinetic model thus needs to cover, in addition to a wide temperature range, all degrees of conversion. Under these circumstances, it is clear that relatively minor amounts of species of different reactivity may undermine the fit of the model. Furthermore, the available kinetic models (such as the ones in Table 1.1) may prove insufficient to describe the conversions of real materials. Models derived for certain limiting cases, which can reasonably describe isothermal data or a portion of the conversion range, may run into problems in describing complete thermograms.

Another issue in kinetic analysis of TPx data is related to the topochemical characteristics, which are common among reactions involving solids. Kinetic analysis of a topochemical

reaction requires, alongside the intrinsic rate law, consideration of the dynamics of the area of the active interface [36]. This means that the initial size and shape of the reactant may play a role in topochemical reactions. In particular, a wide variability in the particle size distribution of the reactant influences the overall kinetics appearing in the thermogram and undermines the utility of an analysis performed with models typically assuming constant particle size. If variability is moderate, on the other hand, models relying on average particle size may be sufficient. Particle size effects are illustrated by Tonge [140], who simulated, for example, the TPR profiles of bimodally distributed powders. Nucleation and nuclei growth models encounter similar difficulties if the reactive material exists in variable size scale.

There is still another special feature related to the kinetic analysis of typical temperature-programmed reactions. The balance equations of the physico–chemical system of TPx assume the conservation of matter. Thus the total amount of solid reactant in the simulation model must match the value of experiments; that is, in practical terms the simulated and measured thermograms must be equal in area. Consequently, if the model does not fit the data in a certain temperature range, it is destined to fail at a later stage, too. The best-fit model solution is obtained as a compromise over the whole range of degrees of conversion. The differences between a model and experimental TPx data expressed as a function of temperature often display undesired systematic trends.

5.3. Methodological remarks

Isoconversional and model-free methods

Methodological aspects of kinetic analysis of solid-state and gas–solid reactions have been a subject of considerable interest during recent years [141-164]. General distrust of some traditional as well as some model-fitting based methods of kinetic analysis has inspired a search for alternative methods that could give consistent results even for complicated solid-state reactions [159, 149, 152, 153]. The isoconversional 'model-free' methods have gained attention in the field of kinetic analysis of thermoanalytical data as a means of determining the activation energy. Isoconversional methods are classified into differential isoconversional methods (the Friedman method [40]) and integral isoconversional methods (the Ozawa–Flynn–Wall method [150] and the Vyazovkin method [148, 149]). The Friedman and Vyazovkin methods are otherwise equal [145], but the latter is more robust to signal noise [161]. While the isoconversional methods do not require an assumption about the reaction

mechanism to produce the activation energies, the NPK (non-parametric kinetics) method, introduced by Serra et al. [152], assumes even less and aims only at providing predictions of the reaction rates. The NPK method regresses experimental data by assuming that a reaction rate is a product of a temperature-dependent and a conversion dependent function [152]. The NPK method has been discussed by Sempere et al [153], Sewry et al. [154] and Opfermann et al. [155,156], but has not yet been introduced for many applications.

The isoconversional model-free methods are advocated for their ability to provide estimates of activation energy independent of reaction mechanisms [147]. The essence of the isoconversional methods is acknowledgment of the complex nature of an overall solid-phase reaction and the inexpressibility of the activation energy as a single constant [147]. There are some controversial aspects in regard to the utility of these methods, however. Vyazovkin [147,165,157] suggests accepting the concept of *effective* activation energy, which could vary with the degree of conversion or temperature or both. The effective activation energy is the 'combined' activation energy for the overall process possibly comprising multiple chemical (or physical) rate processes. However, this effective activation energy does not represent the fundamental activation barrier of the reaction, related to the redistribution of the chemical bonds [158,159].

The isoconversional methods typically produce the activation energy as a function of degree of conversion. The interpretation of possible variable activation energy in physico-chemical terms poses serious difficulties. The overall reaction may involve one composite serial reaction, where the rate-controlling steps change with the reaction conditions. Or it may involve multiple parallel reactions with different reacting species or multiple parallel mechanisms for one reacting species. There are numerous other examples of overlapping chemical and/or physical elementary processes contributing to the overall dynamics. While the results of the isoconversional methods surely indicate possible complexity, they give no information regarding the origins of that complexity. Isoconversional methods also ignore the influence of the pre-exponential factor and give absolutely no information on the reaction mechanism. The resulting activation energy values as a function of degree of conversion may also be confusing, since they are not directly related to the microkinetic activation barriers of the individual steps. Furthermore, it may not be sufficient to report the effective activation energy as a function of conversion since the effective activation energy as obtained from the

isoconversional methods generally is also a function of temperature. This can be illustrated with a simple example.

Consider a hypothetical reaction that involves decomposition of one reactant via two independent parallel mechanisms, where the rate of decomposition is expressed as

$$\frac{d\alpha}{dt} = k_1(T)\, f_1(\alpha) + k_2(T)\, f_2(\alpha)\,, \tag{5.1}$$

The effective activation energy, as understood in isoconversional methods, is analytically:

$$E_\alpha = \frac{E_1 k_1(T)\, f_1(\alpha) + E_2 k_2(T)\, f_2(a)}{k_1(T)\, f_1(\alpha) + k_2(T)\, f_2(a)} \tag{5.2.}$$

Let us now assign parameters and mechanisms for eq. (5.1): $f_1(\alpha)=1-\alpha$, $f_2(\alpha)=(1-\alpha)^2$, $A_1=1*10^{16}$ 1/min, $A_2=1*10^{8}$ 1/min, $E_1=200$ kJ/mol and $E_2=100$ kJ/mol, as in ref. [145]. Model (5.1) with these mechanism and parameter selections represents a composite process with two highly overlapping subprocesses. Figure 5.1 a) illustrates the effective activation energy (eq. (5.2)) as a function of temperature and the degree of conversion. While the conversion–temperature trajectory of the process is unique for each heating rate (Fig. 5.1. b. for the example process), the effective activation energy as obtained with isoconversional methods is dependent on the applied set of heating rates. Figure 5.2 demonstrates calculated effective activation energies for the example process obtained by applying the isoconversional method and using three sets of heating rates. The results shown in Fig. 5.2 differ very clearly, even though the example process was not particularly complex. Effective activation energy as determined by isoconversional methods is thus a quantity of empirical nature, the reporting of which should be accompanied by a report of the heating rates and starting temperatures.

Galwey [158] has discussed analytically different factors that may cause variable activation energy and regards this as a composite parameter in which the contributions from several controls remain undistinguished. He rejects the determination of effective activation energy and proposes that reliable kinetic predictions should be based on constant value activation energies associated with the contributory processes [158].

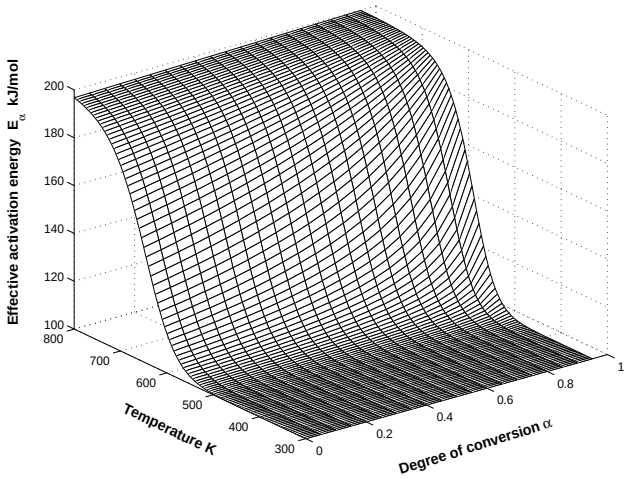

Figure 5.1. a) Effective activation energy as a function of temperature and degree of conversion.

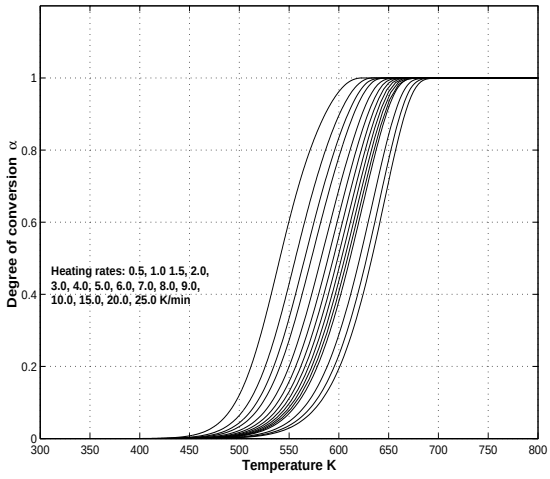

b) Conversion–temperature curves with different heating rates.

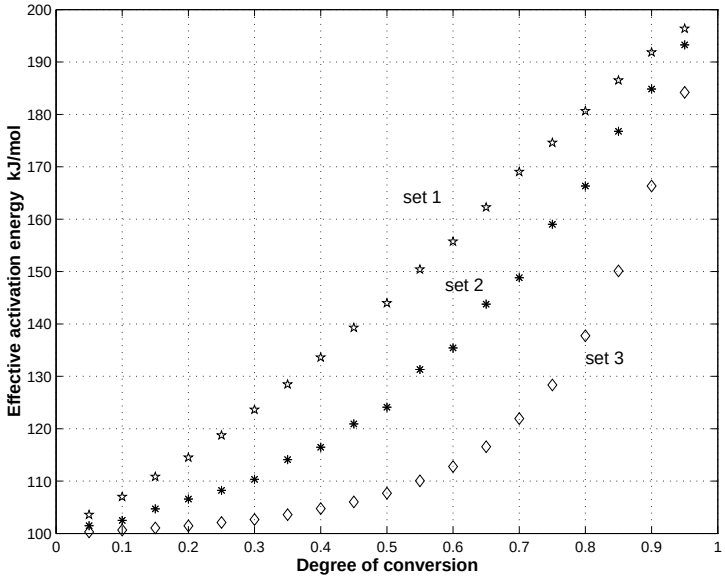

Figure 5.2. Effective activation energy as a function of reduction degree as obtained by applying three sets of heating rates: set 1=10, 15, 20, 25 K/min; set 2=3, 5, 7, 9 K/min; set 3= 0.5, 1.0, 1.5, 2 K/min.

If the isoconversional analysis results in a constant activation energy, as a function of degree of conversion, the reaction rate is presumably limited by a single rate determining step and it should be easy to discover the pre-exponential factor and the reaction mechanism. On the other hand, if the resulting activation energy varies with the conversion, then most simple mechanistic explanations are ruled out and it is useless to carry out model fitting with a single-step unidirectional reaction rate model either. Evidently then, isoconversional methods do not contribute to an understanding of the underlying chemical phenomena.

The utility of these methods remains an on/off measure of the simplicity/complexity of the examined reaction and the isoconversional and NPK methods only postpone the inevitable determination of a kinetic model.

Methods of kinetic analysis based on model fitting and mechanism and parameter identifiability

Some of the distrust of model-fitting based methods originates from the application of temperature-programmed data, the information content of which does not ensure proper identifiability, and also from the force-fitting of unidirectional single-step rate models in situations that call for more complex description.

Kinetic analysis of temperature-programmed experiments by model fitting confronts two identiafibility challenges: identifiability of the mechanism and identifiability of the parameters. The former involves distinguishing a unique functional form of the kinetic model. Basically, as transient techniques, the TPx methods should provide better mechanism identifiability than static experiments. The parameter identifiability involves determining the kinetic parameters of a given model from a given set of data. Parametric correlations often arise in modelling of reaction kinetics. The kinetic compensation effect (KCE), the correlation between two Arrhenius parameters of a rate coefficient, is a well-known phenomenon [146, 166] in chemical kinetics. It is customarily minimised by introducing temperature centring to the rate coefficient: $k(T) = A_{ref} \exp(E/R(1/T\text{ref}-1/T))$ and by estimating the less-correlated A_{ref} and E. This is also a useful practise for kinetic modelling of temperature-programmed reactions. A wide temperature range applied in experimenting facilitates the identification of Arrhenius parameters.

The mechanism and parameter identifiability are sometimes partly interconnected. If for an isothermal experiment the rate law is of the simple form

$$\frac{d\alpha}{dt} = k(T)\, f(\alpha), \tag{5.3}$$

the rate coefficient k is naturally separated from the function $f(\alpha)$, since only the latter varies, while k remains constant. A single nonisothermal experiment provides information on both $f(\alpha)$ and $k(T)$ but not in separated form. The adjustable Arrhenius parameters are able to compensate to a certain extent for the function $f(\alpha)$. For this reason, several different

functions $f(\alpha)$ may sometimes satisfactorily fit the data and the mechanism identifiability is poor. For example, the models of class

$$f(\alpha) = n(1-\alpha)(-\ln(1-\alpha))^{(n-1)/n} \tag{5.4}$$

irrespective of the value of n are especially capable of representing closely one another's dynamic behaviour if the Arrhenius parameters are suitably adjusted. The contributions of the rate coefficient $k(T)$ and the function $f(\alpha)$ to the reaction rate can be *decoupled* in TPx methods, however, by simultaneously using thermograms obtained with different heating rates as a basis of kinetic modelling. Good mechanism identifiability is commonly achieved by utilising three or four heating rates (I-V). This has been agreed on by many kineticists [163, 161].

Despite the popularity of isoconversional methods applied to thermoanalytical data, true kinetic analysis must involve establishing a kinetic model and determining all its parameters. Reporting the activation energy alone does not constitute kinetic analysis. The value is meaningless until related to a mechanistic model and other kinetic parameters. Independent system variables should account for different reaction conditions while the kinetic parameters should be as condition-independent and material-related as possible. The application of nonlinear regression analysis, based on an adequate physico-chemical description of the investigated system, is thus the most universal method of kinetic analysis. Among the methods of kinetic analysis now available it is the only one that can contribute to a fundamental understanding of rates of gas–solid reactions.

6 CONCLUDING REMARKS

This thesis comprises four case studies on temperature-programmed reactions and the present summary. The work demonstrates that catalyst characterisation data obtained with temperature-programmed experiments can support detailed kinetic analysis of reduction, desorption and oxidation. In each case study, a phenomenological kinetic model was established and the parameters of the model were determined by nonlinear regression analysis.

Kinetic modelling substantially extends the interpretability of temperature-programmed reaction data for characterising heterogeneous catalysts. The results of kinetic analysis facilitate the comparison of catalyst characterisation information obtained under different reaction conditions by different research groups. Kinetic analysis of temperature-programmed reactions is also a potentially useful tool in microkinetic analysis of heterogeneously catalysed reactions, especially when the elementary reactions can be probed separately. If the adsorption/desorption or the reduction/oxidation kinetics of the reactants or the products relevant to the total reaction can be determined separately, the credibility of the total microkinetic model is improved ("divide and conquer"). The approaches introduced in this work can be applied to obtain fundamental information on gas–solid interactions or to construct models to provide predictions for assisted catalyst design or process engineering.

REFERENCES

1. Thomas, J. M., Thomas, W. J., *Principles and Practice of Heterogeneous Catalysis*, WCH Verlag GmbH, Weinheim, 1997.
2. Kobayashi, H., Kobayashi, M., Transient response method in heterogeneous catalysis, *Catal. Rev. – Sci. Eng.* **10** (1974) 139-176.
3. Furusawa,T., Suzuki, M., Smith, J. M., Rate parameters in heterogeneous catalysis by pulse techniques, *Catal. Rev. – Sci. Eng.* **13** (1976) 43-76.
4. Bennett, C. O., The transient method and elementary steps in heterogeneous catalysis, *Catal. Rev. – Sci. Eng.* **13** (1976) 121-147.
5. Bennett, C. O., Experiments and processes in the transient regime for heterogeneous catalysis, Adv. Catal. **44** (2002) 329-416.
6. Tamaru, K., *Dynamic Heterogeneous Catalysis*, Academic Press, New York, 1978.
7. Mills, P.L., Lerou, J.L., Transient response methods for assisted design of gas phase heterogeneous catalysts: experimental techniques and mathematical modelling, *Catal. Rev. – Sci. Eng.* **9** (1993) 1-96.
8. Kobayashi, M., Characterization of transient response curves in heterogeneous Catalysis—I Classification of the curves, *Chem. Eng. Sci.* **37** (1982) 393-401.
9. Müller, E., Hofmann, H., Dynamic modelling of heterogeneous catalytic reactions – I. Theoretical considerations, *Chem. Eng. Sci.* **42** (1987) 1695-1704.
10. Salmi, T., Modelling and simulation of transient states of ideal heterogeneous catalytic reactors, *Chem. Eng. Sci.* **43** (1988) 503-511.
11. Renken, A., Transient operation for the purpose of modeling heterogeneous catalytic reactions, *Int. Chem. Eng.* **33** (1993) 61-71.
12. Pekar, M., Koubek, J., Rate-limiting step. Does it exist in the non-steady state?, *Chem. Eng. Sci.* **52** (1997) 2291-2297.
13. Pekar, M., Koubek, J., On general principles of transient behaviour of heterogeneous catalytic reactions, *Appl. Catal., A* **199** (2000) 221-226.
14. Belohlav, Z., Zamostny, P., A rate-controlling step in Langmuir-Hinshelwood kinetic models, *Can. J. Chem. Eng.* **78** (2000) 513-521.
15. Zamostny, P., Belohlav, Z., Identification of kinetic models of heterogeneously catalysed reactions, *Appl. Catal., A* **225** (2002) 291-299.
16. Dekker, F. H. M., Bliek, A., Kapteijn, F., Moulijn, J. A., Analysis of mass and heat transfer in transient experiments over heterogeneous catalysts, *Chem. Eng. Sci.* **50** (1995) 3573-3580.
17. Gleaves, J. T., Ebner, J. B., Kueschler, T. C., Temporal analysis of products (TAP) - a unique catalyst evaluation system with submillisecond time resolution, *Catal. Rev. – Sci. Eng.* **30** (1988) 49-116.
18. Happel, J., Isotopic Assessment of Heterogeneous Catalysis, Academic Press, Orlando, 1986.
19. Mirodatos, C., Use of isotopic transient kinetics in heterogeneous catalysis, *Catal. Today* **9** (1991) 83-95.
20. van der Linde, S. C., Nijhuis, T. A., Dekker, F. H. M., Kapteijn, F., Moulijn, J. A., Mathematical treatment of transient kinetic data: combination of parameter estimation with solving the related partial differential equations, *Appl. Catal., A* **151** (1997) 27-57.
21. Applied Catalysis, A 151 (1997), Special Issue "Transient Kinetics".
22. Applied Catalysis, A 160 (1997), Special Issue "Kinetic methods in Heterogeneous Catalysis".

23. G. F. Froment, K. C. Waugh (Eds.), Reaction kinetics and the development and operation of catalytic processes, Stud. Surf. Sci. Catal. 133, Elsevier, Amsterdam, 2001.
24. Sestak, J., Satava V., Wendlandt, W. W., The study of heterogeneous processes by thermal analysis, *Thermochim. Acta* **7** (1973) 333-556.
25. Amenomiya, Y., Cvetanovic, R. J., Application of flash-desorption method to catalyst studies. III. Propylene alumina system and surface heterogeneity, *J. Phys. Chem.* **67** (1963) 2705-2708.
26. Redhead, P. A., Thermal desorption of gases, *Vacuum* **12** (1962) 203-201.
27. Robertson, S. D., McNicol, B. D., De Baas, J. H., Kloet S. C., Jenkins, J. W., Determination of reducibility and identification of alloying in copper–nickel-on-silica catalysts by temperature-programmed reduction, *J. Catal.* **37** (1975) 424-431.
28. Kapteijn, F., Moulijn, J. A., Tarfaoui, A., Catalyst characterization and mimicking pre-treatment procedures by temperature-programmed techniques, In *Catalysis: An Integrated Approach*, Vol. 123 of *Stud. Surf. Sci. Catal.*, Elsevier, Amsterdam 1999, pp. 525-541.
29. Cvetanovic, R. J., Amenomiya, Y., Temperature programmed desorption technique for investigation of practical catalysts, *Catal. Rev.* **6** (1972) 21-48.
30. Falconer, J. L., Schwarz, J. A ., Temperature-programmed desorption and reaction: applications to supported catalysts, *Catal. Rev.– Sci. Eng.* **25** (1983) 141-227.
31. Hurst, N. W., Gentry, S. J., A. Jones, Temperature-programmed reduction, *Catal. Rev. –Sci. Eng.* **24** (1982) 233-309.
32. Lemaitre, J.L., Temperature-programmed methods, In *Characterization of Heterogeneous Catalysts*, Ed. Delannay, F., Marcel Dekker, Inc., New York 1984, pp. 29-70.
33. Jones, A., McNicol, B., *Temperature-Programmed Reduction for Solid Materials Characterization*, Marcel Dekker Inc., New York, 1986.
34. Bhatia, S., Beltramini, I., Do, D. D., Temperature-programmed analysis and its applications in catalytic systems, *Catal. Today* **7** (1990) 309-438.
35. Tyynelä, N., *Kinetics of reduction of CrO_x/Al_2O_3*, Master's Thesis, in Finnish, Helsinki University of Technology, Espoo, 2000.
36. Haber, J., Kinetics and mechanism of the reduction of VIb transition metal oxides and their oxysalts, *J. Less-Comm. Met.* **54** (1977) 243-261.
37. Brown, M. E., Dollimore, D., Galwey, A. K., Reactions in the solid state, In *Comprehensive Chemical Kinetics*, Eds. Bamford, C. H., Tipper, C.F.H., Vol. 22, Elsevier, Amsterdam 1980, pp. 340.
38. Galwey, A. K., Brown, M. E., Application of the Arrhenius equation to solid state kinetics: can this be justified?, *Thermochim. Acta* **386** (2002) 91-98.
39. Kissinger, H.E., Reaction kinetics in differential thermal analysis, *Anal. Chem.* **29** (1957) 1702-1706.
40. Friedman, H. L., Kinetics of thermal degradation of char-foaming plastics from thermogravimetry — Application to a phenolic resin, *Polym. Sci.* **6C** (1963) 183-195.
41. Senum, G. I., Yang, R. T., Rational approximation of the integral of the Arrhenius function, *J. Thermal Anal.* **11** (1979) 445-447.
42. Bard, Y., *Nonlinear Parameter Estimation*, Academic Press, NewYork, 1974.
43. Bates, D. M., Watts, D. G., *Nonlinear Regression Analysis and its Applications*, John Wiley & Sons, USA, 1988.
44. Seber, G. A. F., Wild, C. J., *Nonlinear Regression*, John Wiley & Sons, USA, 1989.

45. Walter, E., Pronzato, L., *Identification of Parametric Models from Experimental Data*, Springer, Great Britain,1997.
46. Haber, J., Oxidation of hydrocarbons, In *Handbook of Heterogeneous Catalysis*, Eds. G. Ertl, H. Knözinger, J. Weitkamp, Vol. 5, VCH, Weinheim 1997, pp. 2253.
47. Knötzinger, H., Temperature-programmed reduction, In *Handbook of Heterogeneous Catalysis*, Eds. Ertl, G., Knözinger, H., Weitkamp, J., Vol. 2, VCH, Weinheim 1997, pp. 676.
48. Wimmers, O. J., Arnoldy, P., Moulijn, J. A., Determination of the reduction mechanism by temperature-programmed reduction: application to small Fe_2O_3 particles, *J. Phys. Chem.* **90** (1986) 1331-1337.
49. Tarfaoui, A., *Modelling the kinetics of reduction by temperature programming*, Ph.D. thesis, Delft University of Technology, The Netherlands, 1996.
50. Monti, D. A. M., Baiker, A., Temperature-programmed reduction. Parametric sensitivity and estimation of kinetic parameters, *J. Catal.* **83** (1983) 323-335.
51 . Malet, P., Caballero, A., The selection of experimental conditions in temperature-programmed reduction experiments, *J. Chem. Soc., Faraday Trans.* **84** (1988) 2369-2375.
52 . Ehrhard, K., Richter, M., Roost, Öhlmann, G., Temperature-programmed reduction of chromium impregnation catalysts: mathematical treatment of complex reduction profiles, *Appl. Catal.* **17** (1985) 23-45.
53. Weckhuysen, B. M., Wachs, I. E., Schoonheydt, R. A., Surface chemistry and spectroscopy of chromium in inorganic oxides, *Chem. Rev.* **96** (1996) 3327-3349.
54. Wachs, I. E., Weckhuysen B. M., Structure and reactivity of surface vanadium oxide species on oxide supports, *Appl. Catal., A* **157** (1997) 67-90.
55. Avrami, M., Kinetics of phase change. I General theory, *J. Chem. Phys.* **7** (1939) 1103-1113.
56. Avrami. M., Kinetics of phase change. II Transformation-time relations for random distribution of nuclei, *J. Chem. Phys.* **8** (1940) 212-224.
57. Avrami, M., Kinetics of phase change. III Granulation, phase change, and microstructures, *J. Chem. Phys.* **9** (1941) 177-184.
58. Sessa, V., Fanfoni, M., Tomellini, M., Validity of Avrami's kinetics for random and non-random distributions of germs, *Phys. Rev., B* **54** (1996) 836-841.
59. Pineda, E., Pradell T., Crespo, D., Non-random nucleation and the Avrami kinetics, *Phil. Mag., A* **82** (2002) 107-121.
60. Fanfoni, M., Tomellini, M., Volpe, M., Treatment of phantom overgrowth in the Kolmogorov-Johnson-Mehl-Avrami kinetics as a correlation problem, *Phys. Rev., B* **5** (2002) 172301.
61. Stobbe-Kreemers, A. W., van Leerdam G. C., Jacobs, J.-P., Brongersma, H. H., Scholten, J. J. F., Characterisation of γ-alumina-supported vanadium oxide monolayers, *J. Catal.* **152** (1995) 130-136.
62. Blasco, T., Galli, A., Lopez Nieto, J. M., Trifiro, F., Oxidative dehydrogenation of ethane and n-Butane on VO_x/Al_2O_3 catalysts, *J. Catal.* **169** (1997) 203-211.
63. Bulushev, D., Kiwi-Minsker, L., Rainone, F., Renken, A., Characterisation of surface vanadia forms on V/Ti-oxide catalyst via temperature-programmed reduction in hydrogen and spectroscopic methods, *J. Catal.* **205** (2002) 115-122.
64. Koranne, M. M., Goodwin, J. G., Marcelin, G., Characterisation of silica- and alumina-supported vanadia catalysts using temperature-programmed reduction, *J. Catal.* **148** (1994) 369-377.

65. Cavani F., Koytyrev, M., Trifiro, F., Bartolini, A., Ghisletti, D., Iezzi, R., Santucci, A., Del Piero, G., Chemical and physical characterisation of alumina-supported chromia-based catalysts and their activity in dehydrogenation of isobutene, *J. Catal.* **158** (1996) 236-250.
66. Hakuli, A., Kytökivi, A., Krause, A.O.I., Dehydrogenation of i-butane on CrO_x/Al_2O_3 catalysts prepared by ALE and impregnation techniques, *Appl. Catal., A* **190** (2000) 219-232.
67. Mentasty, L. R., Gorriz, O. F., Cadus, L. E., A study of chromia–alumina interaction by temperature-programmed reduction in dehydrogenation catalysts, *Ind. Eng. Chem. Res.* **40** (2001) 136-143.
68. J. N. Finch, Reduction studies on supported chromic anhydride catalysts, *J. Catal.* **43** (1976) 111-121.
69. Fouad, N., Knözinger, H., Zaki, M., Chromia on silica and alumina catalysts: temperature-programmed reduction and structure of surface chromates, *Z. Phys. Chem.* **186** (1994) 231-244.
70. Zaki, M. I., Fouad, N. E., Bond, G. C., Tahir, S. F., Temperature-programmed reduction of calcined chromia-coated alumina and silica catalysts: probing chromium (VI)-oxygen species, *Thermochim. Acta* **285** (1996) 167-179.
71. Roozeboom, F., Mittelmeijer-Hazeleger, M. C., Moulijn, J. A., Medema, J., de Beer, V. H. J., Gellings, P. J., Vanadium oxide monolayer catalysts 3. A Raman spectroscopic and temperature-programmed reduction study of monolayer and crystal-type vanadia on various supports, *J. Phys. Chem.* **84** (1980) 2783-2791.
72. Bosch, H., Kip, B. J., van Ommen, J. G., Gellings, P. J., Factors influencing the temperature-programmed reduction profiles of vanadium pentoxide, *J. Chem. Soc., Faraday Trans.* **80** (1984) 2479-2488.
73. Ballivet-Tkatchenko, D., Delahay, G., Hydrogen temperature-programmed reduction based on water analysis, application to vanadium pentoxide, *J. Thermal Anal.* **41** (1994) 1141-1151.
74. Centeno, M. A., Benitez, J. J., Malet, P., Carrizosa, I., Odriozola, J. A., In situ temperature-programmed diffuse reflectance infrared Fourier transform spectroscopy (TPDRIFTS) of V_2O_5/TiO_2 catalysts, *Appl. Spectrosc.* **51** (1997) 416-422.
75. Arena, F., Frusteri, F., Parmaliana, A., Structure and dispersion of supported vanadia catalysts. Influence of the oxide carrier, *Appl. Catal., A* **176** (1999) 189-199.
76. Lopez Nieto, J. M., Soler, J., Concepcion, P., Herguido, J., Menendez, M., Santamaria, J., Oxidative dehydrogenation of alkanes over V-based catalysts: influence of redox properties on catalytic performance, *J. Catal.* **185** (1999) 324-332.
77. Haber, J., Kozlowska, A., Kozlowski, R., The structure and redox properties of vanadium oxide surface compounds, *J. Catal.* **102** (1986) 52-63.
78. Sloczynski, J., Kinetics and mechanism of reduction and reoxidation of the alkali promoted vanadia-titania catalysts, *Appl. Catal., A* **146** (1996) 401-423.
79. Bensalem, A., Weckhuysen, B. M., Schoonheydt, R. A., In situ diffuse reflectance spectroscopy of supported chromium oxide catalysts: kinetics of the reduction process with carbon monoxide, *J. Phys. Chem. B* **101** (1997) 2824-2829.
80. Dekker, F. H. M., Klopper, G., Bliek, A., Kapteijn, F., Moulijn, J. A., Modelling the transient kinetics of heterogeneous catalysts. CO-oxidation over supported Cr and Cu, *Chem. Eng. Sci.* **49** (1994) 4375-4390.

81. Cherian, M., Rao, M. S., Yang, W-T, Jehng, J-M, Hirt, A., Deo, G., Oxidative dehydrogenation of propane over Cr_2O_3/Al_2O_3 and Cr_2O_3 catalysts: effects of loading, precursor and surface area, *Appl. Catal., A* **233** (2002) 21-33.
82 . Cherian, M., Rao, M. S., Hirt, A.M., Wachs, I. E., Deo, G., Oxidative dehydrogenation of propane over supported chromia catalysts: influence of oxide supports and chromia loading, *J. Catal.* **211** (2002) 482-495.
83. Bosch, H., Sinot, P. J., Activation energies of the reduction of bulk and supported vanadium pentoxide, *J. Chem. Soc. –Faraday Trans.* **85** (1989) 1425-1437.
84. Argyle, M. D., Chen, K., Bell, A. T., Iglesia, E., Effect of catalyst structure on oxidative dehydrogenation on ethane and propane on alumina-supported vanadia, *J. Catal.* **208** (2002) 139-149.
85. Le Bars, J., Auroux, A., Forissie, M., Vedrine, J. C., Active sites of V_2O_5/γ-Al_2O_3 catalysts in the oxidative dehydrogenation of ethane, *J. Catal.* **162** (1996) 250-259.
86. Argyle, M. D., Chen, K., Bell, A. T., Iglesia, E., Ethane oxidative dehydrogenation pathways on vanadium oxide catalysts, *J. Phys. Chem, B* **106** (2002) 5421-5427.
87. Schwarz, J. A., Falconer, J. L., Application of transient techniques methanation on supported nickel catalysts, *Catal. Today* **7** (1990) 1-92.
88. Tovbin, Y., Theory of adsorption–desorption kinetics on flat heterogeneous surfaces, In *Equilibria and Dynamics of Adsorption on Heterogeneous Solid Surfaces*, Eds. Rudzinski, W., Steele, W. A., Zgrablich, G., Vol. 104 of *Stud. Surf. Sci. Catal.*, Elsevier, New York 1997, pp. 201-284.
89. Gorte, R. J., Temperature-programmed desorption for the characterisation of oxide catalysts, *Catal. Today* **28** (1996) 405-414.
90. Falconer, J.L., Madix, R.J., Desorption rate isotherms in flash desorption analysis, *J. Catal.* **48** (1977) 262-268.
91. de Jong, A. M., Niemantsverdriet, J. W., Thermal desorption analysis: comparative test of ten commonly applied procedures, *Surf. Sci.* **233** (1990) 355-365.
92. Rudzinski, W., Borowiecki, T., Panczyk, T., Dominko, A., On the applicability of Arrhenius plot methods to determine surface energetic heterogeneity of adsorbents and catalysts surfaces from experimental TPD spectra, *Adv. Colloid Interface Sci.* **84** (2000) 1-26.
93. Russell, N. M., Ekerdt, J. G., Nonlinear parameter estimation technique for kinetic analysis of thermal desorption data, *Surf. Sci.* **364** (1996) 199-218.
94. Niemantsverdriet, J.W, *Spectroscopy in Catalysis, An Introduction*, Wiley-WCH Verlag GmbH, Weinheim , 2000.
95. Ibok, E. E., Ollis, D. F., Temperature-programmed desorption from porous catalysts: shape index analysis, *J. Catal.* **66** (1980) 391-400.
96. Herz, R. K., Kiela, J. B., Marin, S. P., Adsorption effects during temperature-programmed desorption of carbon monoxide from supported platinum, *J. Catal.* **73** (1982) 66-75.
97. Rieck, J. S., Bell, A. T., Influence of adsorption and mass transfer effects on temperature-programmed desorption from porous catalysts, *J. Catal.* **85** (1984) 143-153.
98. Gorte, R. J., Design parameters for temperature programmed desorption from porous catalysts, *J. Catal.* **75** (1982) 164-174.
99. Demmin R. A. Gorte, R. J., Design parameters for temperature-programmed desorption from a packed bed, *J. Catal.* **90** (1984) 32-39.

100. Weisz, P. B., Prater, C. D., Interpretation of measurements in experimental catalysis, *Adv. Catal.* **6** (1954) 143-196.
101. Tronconi, E., Forzatti, P., Experimental criteria for diffusional limitations during temperature-programmed desorption from porous catalysts, *J. Catal.* **93** (1985) 197-200.
102. Huang, Y.-J., Xue, J., Schwarz, J. A., Experimental procedures for the analysis of intraparticle diffusion during temperature-programmed desorption from porous catalysts in a flow system, *J. Catal.* **109** (1988) 396-406.
103. Tronconi, E., Forzatti, P., Modelling and experimental verification of TPD from porous catalysts, *Chem. Eng. Sci.* **41** (1986) 2541-2545.
104. Lee, P.-I., Huang, Y.-J., Heydweiller, J. C., Schwarz, J. A, Analysis of temperature-programmed desorption from porous catalysts in a flow system, *Chem. Eng. Comm.* **63** (1988) 205-224.
105. Hinrichsen, O., Rosowski, F., Muhler, M., Ertl, G., Microkinetic analysis of temperature-programmed experiments in a microreactor flow system, *Stud. Surf. Sci. Catal.* **109** (1997) 389-400.
106. Wedler, G., *Chemisorption: An Experimental Approach*, Butterworths, London, 1976, p. 193-194.
107. Christman, K., Schober, O., Ertl, G., Neumann, M., Adsorption of hydrogen on nickel single crystal surfaces, *J. Chem. Phys.* **60** (1974) 4528-4540.
108. Konvalinka, J. A., van Oeffelt, P. H., Scholten, J. J. F., Temperature-programmed desorption of hydrogen from nickel catalysts, *Appl. Catal.* **1** (1981) 141-258.
109. Lee, P. I., Schwarz, J. A., Adsorption–desorption kinetics of H_2 from supported nickel catalysts, *J. Catal.* **73** (1982) 272-287.
110. Weatherbee, G. D., Bartholomew, C. H., Effects of support on hydrogen adsorption/desorption kinetics of nickel, *J. Catal.* **87** (1984) 55-65.
111. Smeds, S., Salmi, T., Lindfors, L. P., Krause, O., Chemisorption and TPD studies of hydrogen on Ni/Al_2O_3, *Appl. Catal., A* **144** (1996) 177-194.
112. Wedler, G., *Chemisorption: An Experimental Approach*, Butterworths, London, 1976, p. 39-41.
113. Prinsloo, J. J., Gravelle, P. C., Volumetric and calorimetric study of the adsorption of hydrogen, at 296 K, on supported nickel and nickel–copper catalysts containing preadsorbed carbon monoxide, *J. Chem. Soc.– Faraday Trans. I* **76** (1980) 512-519.
114. Padberg, G., Smith, J. M., Chemisorption rates by chromatography, *J. Catal.* **12** (1968) 172-182.
115. Damiani, D. E., Valles, E. M., Gigola, Gas chromatographic determination of adsorption–desorption rates, interaction of hydrogen on a nickel catalyst, C. E., *J. Chromatogr.* **196** (1980) 355-366.
116. Sadeghbeigi, R., *Fluid Catalytic Cracking Handbook*, Gulf Publishing Company, Houston, 1995.
117. Hiltunen, J., Niemi, V.M., Lipiäinen, K, Eilos, I., Hagelberg, P., Knuuttila, P., Jääskeläinen K., Majander, J., Röppänen, J., NExCC™ –Novel short contact time catalytic cracking technology, In *Fluid Catalytic Cracking V: Materials and Technological Innovations*, Eds. Occelli and O'Connor, Elsevier, 2001.
118. Li, C., Brown, T. C., Temperature-programmed oxidation of coke deposited by 1-octene on cracking catalysts, *Energy and Fuels* **13** (1999) 888-894.
119. Magnoux, P., Cerqueira, H. S., Guisnet, M., Evolution of coke composition during ageing under nitrogen, *Appl. Catal., A* **235** (2002) 93-99.

120. Fung, S. C., Querini C. A., A Highly sensitive detection method for temperature-programmed oxidation of coke deposits: methanation of CO_2 in the presence of O_2, *J. Catal.* **138** (1992) 240-254.
121. Querini, C. A., Fung, S. C., Coke characterisation by temperature-programmed techniques, *Catal. Today* **37** (1997) 277-283.
122. Querini, C. A., Fung, S. C., Temperature-programmed oxidation technique: kinetics of coke–O_2 reaction on supported metal catalysts, *Appl. Catal.*, A **117** (1994) 53-74.
123. Bayraktar, O., Kugler, E. L., Characterisation of coke on equilibrium fluid catalytic cracking catalysts by temperature-programmed oxidation, *Appl. Catal.*, A **233** (2002) 197-213.
124. Weisz, P. B., Goodwin, R. D., Combustion of carbonaceous deposits within porous catalyst particles I. Diffusion-controlled kinetics, *J. Catal.* **2** (1963) 397-404.
125. Al-Bayaty, S., Acharya, D. R., Hughes, R., Effect of coke deposited on the effective diffusivity of catalyst pellets, *Appl. Catal.*, A **110** (1994) 109-119.
126. Larachi, F., Belkacemi, K., Hamoudi, S., Sayari, A., Kinetics of carbon evolution in temperature-programmed oxidation of carbonaceous laydown deposited on wet oxidation catalysts, *Catal. Today* **64** (2001) 163-177.
127. Gayubo, A. G., Arandes, J. M., Aguayo A. T., Olazar, M., Bilbao, J., Calculation of the kinetics of catalyst regeneration by burning coke following a temperature ramp, *Chem. Eng. J.* **54** (1994) 35-40.
128. Arandes, J. M., Abajo, I., Fernandez, I., Lopez, D., Bilbao, J., Kinetics of gaseous product formation in the coke combustion of a fluidised catalytic cracking catalyst, *Ind. Eng. Chem. Res.* **38** (1999) 3255-3260.
129. Morley, K., De Lasa, H. I., On the determination of kinetic parameters for the regeneration of cracking catalyst, *Can. J. Chem. Eng.* **65** (1987) 773-777.
130. Morley, K., De Lasa, H. I., Regeneration of cracking catalyst: influence of the homogeneous postcombustion reaction, *Can. J. Chem. Eng.* **66** (1988) 428-432.
131. Le Minh, C., Jones, R. A., Craven, I. E., Brown, T. C., Temperature-programmed oxidation of coke deposited on cracking catalysts: combustion mechanism dependence, *Energy and Fuels* **11** (1997) 463-469.
132. Le Minh, C., Li, C., Brown, T. C., Kinetics of coke combustion during temperature-programmed oxidation of deactivated cracking catalysts, Stud. Surf. Sci. Catal. **111** (1997) 383-390.
133. Li, C., Le Minh, C., Brown, T. C., Kinetics of CO and CO_2 evolution during the temperature-programmed oxidation of coke deposited on cracking catalysts, *J. Catal.* **178** (1998) 275-283.
134. Li, C., C., Brown, T. C., Temperature-programmed oxidation of coke deposited by 1-octene on cracking catalysts, *Energy and Fuels* **13** (1999) 888-894.
135. Li, C., C., Brown, T. C., Carbon oxidation kinetics from evolved carbon oxide analysis during temperature-programmed oxidation, *Carbon* **39** (2001) 725-732.
136. Dimitriadis, V. D., Lappas, A. A., Vasalos, I. A., Kinetics of combustion of carbon in carbonaceous deposits on zeolite catalysts for fluid catalytic cracking units (FCCU). Comparison between Pt and non Pt-containing catalysts, *Fuel* **77** (1998) 1377-1383.
137. Weisz, P. B., Goodwin, R. D., Combustion of carbonaceous deposits within porous catalyst particles. II. Intrinsic burning rate, *J. Catal.* **6** (1966) 227-236.
138. Wang, G., Lin, S., Mo, W., Peng C., Yang, G., Kinetics of combustion of carbon and hydrogen in carbonaceous deposits on zeolite-type cracking catalysts, *Ind. Eng. Chem. Process. Dev. Des.* **25** (1986) 626-630.

139. Froment, G. F., Bischoff, K. B., *Chemical Reactor Analysis and Design*, 2nd Ed., John Wiley & Sons, Singapore,1990, p. 82-83.
140. Tonge K. H., Particle size effects in temperature-programmed topochemical reactions, *Thermocim. Acta* **74** (1984) 151-166.
141. Ortega, A., The kinetics of solid-state reactions toward consensus – Part I: uncertainties, failures, and successes of conventional methods, *Int. J. Chem. Kinet.* **33** (2001) 343-353.
142. Ortega, A., The kinetics of solid-state reactions toward consensus – Part 2: fitting kinetics data in dynamic conventional thermal analysis, *Int. J. Chem. Kinet.* **34** (2002) 193-208.
143. Ortega, A., The kinetics of solid-state reactions toward consensus – Part 3: searching for consistent kinetics results: SCTA vs. conventional thermal analysis, *Int. J. Chem. Kinet.* **34** (2002) 223-236.
144. Budrugeac, P., Segal, E., Some methodological problems concerning nonisothermal kinetic analysis of heterogeneous solid–gas reactions, *Int. J. Chem. Kinet.* **33** (2001) 564-573.
145. Vyazovkin, S., Some confusions concerning integral isoconversional methods that may result from the paper by Budrugeac and Segal "Some methodological problems concerning nonisothermal kinetic analysis of heterogeneous solid–gas reactions", *Int. J. Chem. Kinet.* **34** (2002) 418-420.
146. Brown, M. E., Galwey, A. K., The significance of "compensation effects" appearing in data published in "computational aspects of kinetic analysis" ICTAC project, 2002, *Thermochim. Acta* **387** (2002) 173-183.
147. Vyazovkin, S., Kinetic concepts of thermally stimulated reactions in solids: a view from historical perspective, *Int. Rev. Phys. Chem.* **19** (2000) 45-60.
148. Vyazovkin, S., Dollimore, D., Linear and nonlinear procedures in isoconversional computations of the activation energy of nonisothermal reactions in solids, *J. Chem. Inf. Comput. Sci.* **36** (1996) 42-45.
149. Vyazovkin, S., Evaluation of activation energy of thermally stimulated solid-state reactions under arbitrary variation of temperature, *J. Comput. Chem.* **18** (1997) 393-402.
150. Ozawa, T., A new method of analyzing thermogravimetric data, *Bull. Chem., Soc., Jpn.* **38** (1965) 1881-1886; Flynn , J. H., Wall, L. A. J., General treatment of the thermogravimetry of polymers, Res. Natl. Bur. Stand. (US) 70A (1966) 487-523.
151. Sbirrazuoli, N., Vincent, L., Vyazovkin, S., Comparison of several computational procedures for evaluating the kinetics of thermally stimulated condensed phase reactions, *Chem. Intel. Lab. Systems* **54** (2000) 53-60.
152. Serra, R., Sempere, J., Nomen, R., A new method for the kinetic study of thermoanalytical data: the non-parametric kinetics method, *Thermochim. Acta* **316** (1998) 37-45.
153. Sempere J., Nomen, R., Serra, J., Soravilla, J., The NPK method: an innovative approach for kinetic analysis of data from thermal analysis and calorimetry, *Thermochim. Acta* **388** (2002) 407-414.
154. Sewry, J. D., Brown, M. E., "Model-free" kinetic analysis?, *Thermochim. Acta* **390** (2002) 217-225.
155. Opfermann, J. R., Kaiserberger, E., Flammersheim, H.-J., Model-free analysis of thermoanalytical data – advantages and limitations, *Thermochim. Acta* **391** (2002) 119-127.

156. Opfermann, J. R., Flammersheim H.-J., Some comments to the paper of J. D. Sewry and M. E. Brown: "Model-free" kinetic analysis?, *Thermochim. Acta* **397** (2003) 1-3.
157. Vyazovkin, S., Reply to "What is meant by the term 'variable activation energy' when applied in the kinetics analyses of solid state decompositions (crystolysis reactions)?", *Thermochim. Acta* **397** (2003) 269-271.
158. Galwey, A. K., What is meant by the term 'variable activation energy' when applied in the kinetics analyses of solid state decompositions (crystolysis reactions)?, *Thermochim. Acta* **397** (2003) 249-268.
159. Vyazovkin, S., Wight, C. A., Kinetics in solids, *Annu. Rev. Phys. Chem.* **48** (1997) 125-149.
160. Brown, M. E., Maciejewski, M., Vyazovkin, S, Nomen, R., Sempere, J., Burnham, A., Opfermann, J., Strey, R., Anderson, H. L., Kemmler, A., Keuleers, R., Janssens, J., Desseyn, H. O., Li, C.-R., Tang, T. B., Roduit, B., Malek, J., Mitsuhashi, T., Computational aspects of kinetic analysis Part A: the ICTAC kinetics project—data, methods and results, *Thermochim. Acta* **355** (2000) 125-143.
161. Maciejewski, M., Computational aspects of kinetic analysis Part B: the ICTAC kinetics project – the decomposition kinetics of calcium carbonate revisited, or some tips on survival in the kinetic minefield, *Thermochim. Acta* **355** (2000) 145-154.
162. Vyazovkin, S., Computational aspects of kinetic analysis Part C: the ICTAC kinetics project – the light at the end of the tunnel, *Thermochim. Acta* **355** (2000) 155-163.
163. Burnham, A. K., Computational aspects of kinetic analysis Part D: the ICTAC kinetics project – multi-thermal-history model-fitting methods and their relation to isoconversional methods, *Thermochim. Acta* **355** (2000) 165-170.
164. Roduit, B., Computational aspects of kinetic analysis Part E: the ICTAC kinetics project – numerical techniques and kinetics of solid state processes, *Thermochim. Acta* **355** (2000) 171-180.
165. Vyazovkin, S., On the phenomenon of variable activation energy for condensed phase reactions, *New J. Chem.* **24** (2000) 913-917.
166. Bond, G. C., Keane, M. A., Kral, H., Lercher, J. A., Compensation phenomena in heterogeneous catalysis: general principles and a possible explanation, *Catal. Rev. – Sci. Eng.* **42** (2000) 323-282.